EMISSIONS COMPARISON BETWEEN PETROLEUM DIESEL AND BIODIESEL IN A MEDIUM-DUTY DIESEL ENGINE

A Thesis

by

BRANDON T. TOMPKINS

Submitted to the Office of Graduate Studies of
Texas A&M University
in partial fulfillment of the requirements for the degree of

MASTER OF SCIENCE

December 2008

Major Subject: Mechanical Engineering

EMISSIONS COMPARISON BETWEEN PETROLEUM DIESEL AND BIODIESEL IN A MEDIUM-DUTY DIESEL ENGINE

A Thesis

by

BRANDON T. TOMPKINS

Submitted to the Office of Graduate Studies of
Texas A&M University
in partial fulfillment of the requirements for the degree of

MASTER OF SCIENCE

Approved by:

Chair of Committee,	Timothy Jacobs
Committee Members,	Warren Heffington
	Kenneth R. Hall
Head of Department,	Dennis O'Neal

December 2008

Major Subject: Mechanical Engineering

ABSTRACT

Emissions Comparison between Petroleum Diesel and Biodiesel in a Medium-Duty Diesel Engine. (December 2008)

Brandon T. Tompkins, B.S., Clemson University

Chair of Advisory Committee: Dr. Timothy Jacobs

Biofuels have become very important topics over the past decade due to the rise in crude oil prices, fear of running out of crude oil, and environmental impact of emissions. Biodiesel is a biofuel that is made from plant seed oils, waste cooking oils, or animal fats. It has become increasingly popular and is looked at as a diesel replacement. This research characterizes the emissions of the new John Deere PowerTech Plus 4045HF285 in the Advance Engine Research Laboratory at Texas A&M University and compares the emissions of a 100 percent blended feed stock biodiesel to an ultra low sulfur diesel certification fuel.

The steady state tests were conducted while holding engine speed constant at three different speeds and three different loads. The gaseous emissions, exhaust gas recirculation, fuel flow rate, and torque were monitored and recorded for 300 points per test. Four tests were performed and the results were averaged per each fuel. Carbon monoxide, carbon dioxide, oxygen, and oxides of nitrogen emissions were analyzed. The biodiesel averaged up to 12% lower torque, 5.4% more fuel, 7.5% less carbon dioxide, 29% more oxygen, and 29% more oxides of nitrogen. Overall the biodiesel produced less torque and carbon dioxide emissions, while emitting more oxygen and oxides of nitrogen.

DEDICATION

To my family, thanks for your support.

ACKNOWLEDGEMENTS

I would like to thank God for my life, health, and strength. I thank Dr. Jacobs, my committee chair, for giving me the opportunity to perform engine research and for his guidance and support. I would also like to thank Dr. Heffington and Dr. Hall for their guidance throughout my time here at Texas A&M University.

Thanks to my laboratory associates (especially Jason and Jesse) and the Mechanical Engineering Machine Shop (Mike and William); this research effort would not have been possible without their help.

Lastly, I would like to extend my gratitude to my father and my future wife; there would have been no way I could have made it this far without their love and support.

NOMENCLATURE

B100	100% Biodiesel
CC	Cubic Centimeter
CO	Carbon Monoxide
CO_2	Carbon Dioxide
ECU	Electronic Control Unit
EGR	Exhaust Gas Recirculation
g/s	Grams Per Second
kg/m^3	Kilograms Per Meters Cubed
kW	Kilowatts
MJ/kg	Mega Joules Per Kilogram
N*m	Newton- Meter
NO	Nitric Oxide
NO_X	Oxides of Nitrogen
NPT	National Pipe Thread
PPM	Parts Per Million
O_2	Oxygen
RPM	Revolutions Per Minute
VGT	Variable Geometry Turbocharger

TABLE OF CONTENTS

Page

Page

LIST OF FIGURES

Page

Page

Page

LIST OF TABLES

Page

1 INTRODUCTION

As emission standards go lower and lower, and oil prices keep rising, there is a need for a petroleum substitute in both compression and spark ignition engines. Many promising sources have been discovered including alcohol derived fuels and synthetic fuels. Biodiesel has emerged as a promising diesel substitute; however, it has its own share of problems. The biodiesel "NO_x Effect" has yet to be solved. Characteristic of biodiesel needs to be fundamentally investigated by looking at fuel. Previous studies show that biodiesel produces more NO_x than petroleum diesel. This potential characteristic of biodiesel needs to be fundamentally investigated by investigating several features including fuel properties, injection and combustion characteristics; this research focuses on the initial comparison and characterization of the exhaust data from the two fuels.

Diesel engines have been around for over a hundred years. They are used in cars, trucks, tractors, heavy machinery, ships, numerous military vehicles, and power generation applications. The diesel engine is practically perceived to be more durable than the gasoline engine in that it does not require an external ignition system and its components are more heavily built; they commonly last 250,000 vehicle miles or more without the need to be rebuilt. Diesel engines also conventionally obtain better fuel economy than gasoline engines of the same power rating, a fact that is making them very popular in the auto industry now. One of the major obstacles challenging the use of the

---

This thesis follows the style of The Journal for Engineering of Gas Turbines and Power.

diesel engine is its emission characteristics. Diesel engines emit large amounts of particulate matter, carbon dioxide, and nitric oxides. This is a problem because particulate matter poses a serious risk to health as stated by the Environmental Protection Agency. Carbon dioxide is a major greenhouse gas and, nitric oxide is one the main contributors to tropospheric ozone formation and to acid rain. The scientific community is using different technology to tackle the emissions issue, such as exhaust gas recirculation (EGR), high pressure common rail fuel injection, piezoelectric fuel injectors, variable geometry turbochargers, and exhaust after treatment systems. The scientific community is also using different fuels, such as ultra low sulfur diesel and potentially biodiesel.

Biodiesel is a diesel replacement that is prepared by refining plant seed oil, animal fat, or waste cooking oil. Biodiesel is produced by a method called transesterfication. This is done by reacting the oil, fat, or waste cooking oil with an alcohol (mainly methanol, or ethanol), along with an alkali catalyst to produce methyl or ethyl esters and a glycerol by-product [1]. It is similar to diesel fuel, with the exception of its higher cetane number, higher density, and higher viscosity. Biodiesel is a promising petroleum diesel replacement because it has similar fuel properties as petroleum diesel. It is produced from a renewable energy source and it is biodegradable. One negative characteristic of biodiesel is a lower heating value than diesel, causing it to produce less torque, and consume additional fuel [2]. Another characteristic is it acts as a solvent by cleaning out storage containers and dissolving hoses. Biodiesel produces about 18% less carbon dioxide (CO_2) and about the same carbon monoxide (CO) as

diesel; the nitric oxide emissions, however, are increased to about 11% when using 100% biodiesel [3]. This increase in nitric oxides is known as the "NOx Effect", and there are many different causes that have been investigated. One of the causes was found to be the advanced injection timing of biodiesel compared to regular diesel. The injection timing is important because it has a direct affect on the ignition delay. Ignition delay is the time between the start of injection and start of combustion. Some properties of the fuel affect the ignition delay, such as cetane number and viscosity. A high cetane number will give a shorter ignition delay; however, a high viscosity could prolong the ignition delay because it gives the fuel poor atomization when injected into the cylinder. This makes the vaporization and mixing process of the fuel with air longer. The viscosity of the fuel affects the injection timing also. Kegl [4], et al. found that high viscosities which reduced the fuel leakage during injection, and a higher bulk modulus of compressibility (the measure of how resistant a substance is to being compressed) lead to a faster rise in pressure that advances the injection timing. Senatore, et al. [5] found that the biodiesel injection timing was advanced by as much as 0.6 crank angles degrees. Szybist, et al. [6] stated that the advance in injection timing was caused by the higher bulk modulus, and that the early needle lift was from the pressure waves traveling from the fuel pump to the injector nozzle at a faster than normal rate. They also came to the conclusion that the importance was not in how high the temperature or pressure became, but where the spike occurred for NO formation in biodiesel. There are many causes that contribute to the biodiesel "NO_x Effect" that are in the injection and

combustion characteristics. No one has discovered a definite way to stop or prevent the "NO_x Effect" from occurring, thus more research is needed on the subject matter.

The objective of this experiment is to compare the emissions of ultra low sulfur reference diesel and a 100% blended feedstock biodiesel in a John Deere PowerTech Plus diesel engine, which features the latest low emissions technology, such as EGR, variable geometry turbocharger (VGT), common rail fuel injection, and piezoelectric fuel injectors. This research will also display the ability to produce repeatable data in the Advanced Engine Research Laboratory. This is a preliminary step in an ongoing investigation of nitric oxide formation in biodiesel emissions.

2 EXPERIMENTAL METHODOLOGY

This experiment was conducted in the Advanced Engine Research Laboratory at Texas A&M University, Figure 1 shows how the lab is setup.

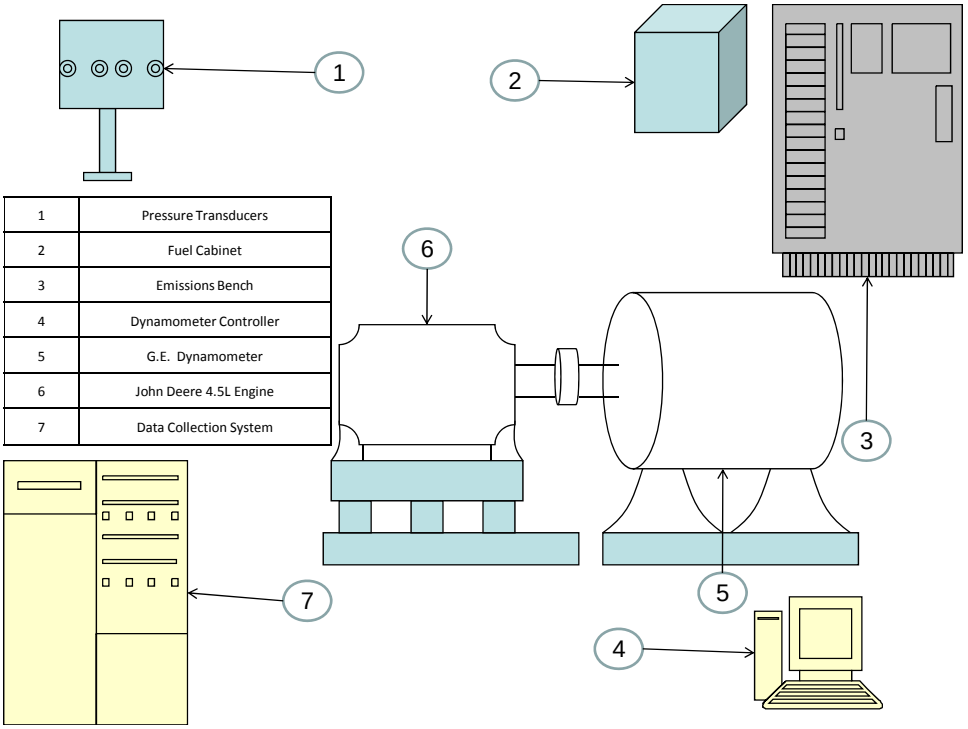

Figure 1: Advanced Research Laboratory Layout

The main purpose of this study is to perform an experiment whose results will show a significant reduction in harmful emissions.

2.1 Engine

The engine used in the study is an inline four cylinder medium-duty Power Tech Plus Series diesel, model 4045HF485 produced by John Deere. It is mainly used for stationary power generation or irrigation. This engine displaces 4.5 liters, has a compression ratio of 17.0:1, and has two intake and exhaust valves per cylinder. It has a power rating of 115k kilowatts (kW) at 2400 rpm and 575 Newton-Meter (N·m) of torque at 1400 rpm. The engine's power and torque curves are shown in Figure 2.

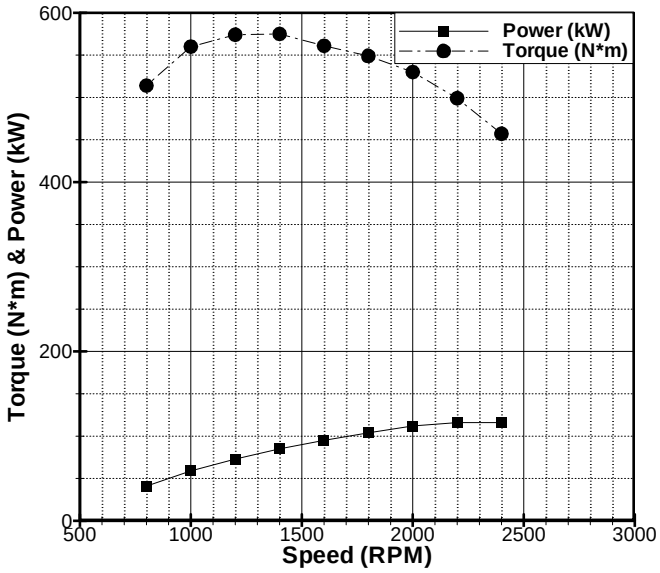

Figure 2: John Deere 4045HF485 Engine Performance Curve

It is equipped with the latest in emission reducing technology, such as high pressure common rail injection, EGR, and a variable geometry turbocharger. Specifications for the engine are provided in Table 1.

Table 1: Engine Specifications

Engine Specification	
Number of Cylinders	**4**
Compression Ratio	**17.0:1**
Bore (in,mm)	**4.19, 106**
Stroke (in,mm)	**5, 127**
Displacement (in^3, L)	**275, 4.5**
Valves per Cylinder Int—Exh	**2—2**
Aspiration	**VGT**
Charge Air Cooling System	**Air-to-Air**
Peak Power (hp, kW @ 2400 rpm)	**154,115**
Peak Torque (ft*lb, N*m @ 1400prm)	**424, 575**
Rated Speed (rpm)	**2400**
Breakaway Speed (rpm)	**2470**
Fast Idle Speed (rpm)	**2600**
BMEP(psi, kpa)	**139, 956**
Friction Power @ Rated Speed (hp, kW)	**28, 21**

Figure 3 shows an example of the common rail fuel injection system placed in John Deere Tier III engines [7].

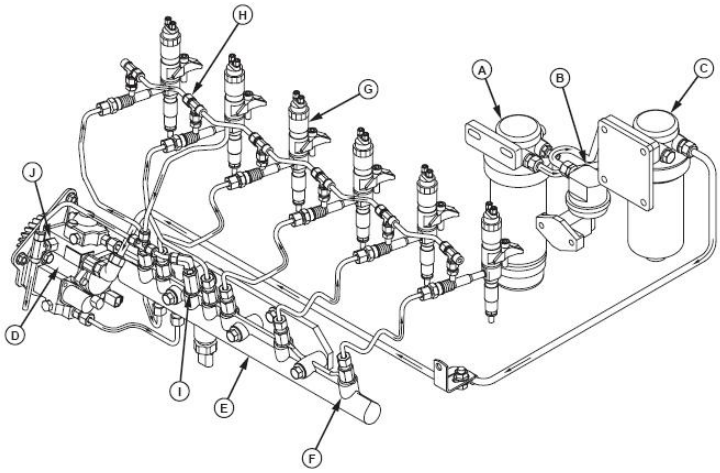

Figure 3: John Deere High Pressure Common Rail Injection System [7]

Common rail fuel injection is the latest in fuel injection systems that are being placed in engines today. It is composed of one fuel rail that feeds all of the injectors and it is fed by a pump that pressurizes up to1800 bar. Figure 4 shows a detailed example of the injectors that make up the common rail system [7].

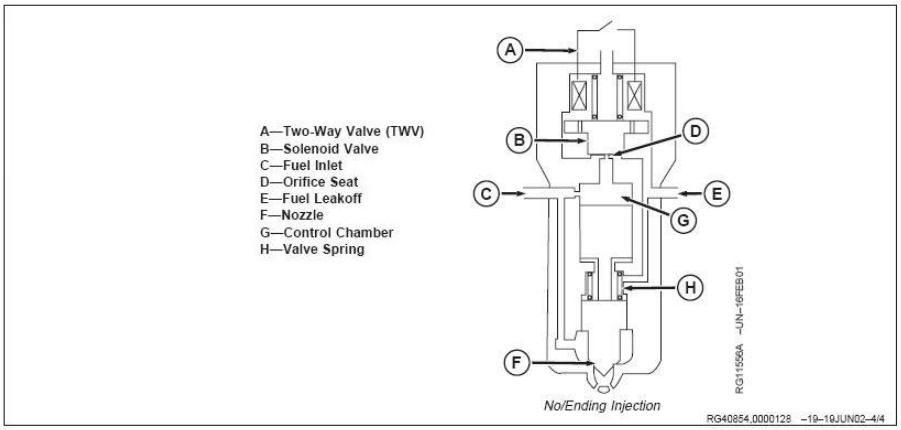

Figure 4: John Deere Piezoelectric Fuel Injector [7]

The injectors are controlled by the engine control unit (ECU). Due to high pressures and precise injection the atomization of the fuel is improved and the fuel burns cleaner helping to reduce emissions.

EGR is a method used to reduce NO_x. The exhaust gas composed of mostly CO_2 and water is pumped from the exhaust manifold through a cooler and then into the intake manifold. Figure 5 shows the flow direction the EGR takes to the intake manifold [7].

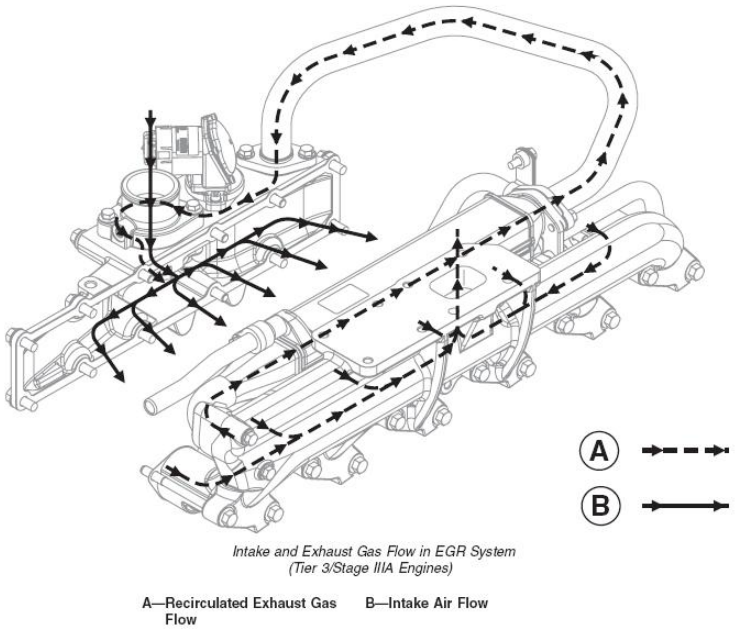

Figure 5: EGR Flow Diagram [7]

EGR dilutes the intake charge, and absorbs energy from the combustion process lowering combustion temperatures, thus reducing NO_x formation.

The VGT serves two purposes: it maintains optimum boost and helps control EGR flow in the engine. The VGT has vanes that are controlled by an actuator that channels flow into the turbine blades. At low speed the vanes close to increase manifold pressure and speed up the turbine. At high speeds, the vanes remain open because the gas has enough energy to turn the turbine blades to create the appropriate boost. EGR is driven by the pressure difference in the exhaust and intake manifolds. The vanes also open and close to create the needed pressure difference to drive the EGR flow. Figure 6 shows an example of how the vane of the turbocharger looks at low and high speeds [8].

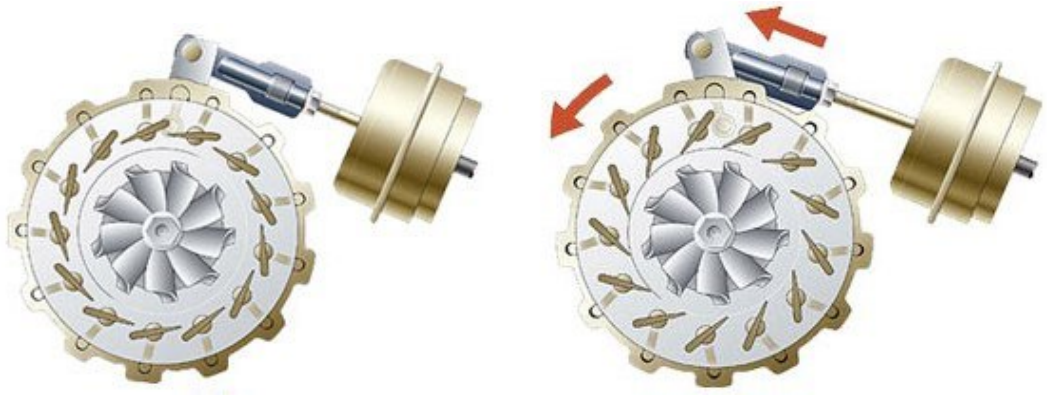

Figure 6: The Vanes of a VGT at Low (left) & High (right) Speeds [8].

2.1.1 Engine Modifications

Modifications were made to three parts of the engine. The intake manifold, exhaust manifold, and exhaust pipe were prepared for temperature and pressure readings. The intake manifold has three quarter-inch national pipe threads (NPT) drilled and tapped for temperature, pressure, and carbon dioxide readings. Two quarter-inch NPT were placed on the exhaust manifold for temperature and pressure measurements. Figure 7 shows the modifications to the intake and exhaust manifolds.

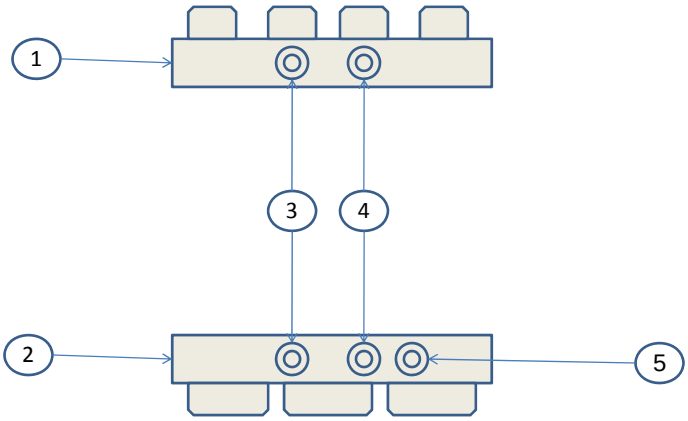

1	Exhaust Mainfold
2	Intake Mainfold
3	Temperature Pipe Fitting
4	Pressure Pipe Fitting
5	Carbon Dioxide Pipe Fitting

Figure 7: Intake and Exhaust Manifold Diagrams

There were eight quarter inch NPT ports welded onto the exhaust pipe; four near the turbocharger and four near the end of the exhaust pipe. Two ports are used for temperature and pressure readings after the turbocharger and one was used at the end of the pipe for emissions sampling.

2.2 Measurements

2.2.1 Pressure and Temperature

All temperature and pressure measurements are made with k-type thermocouples and strain gauge pressure transducers, respectively, as summarized in Table 2.

Table 2: Temperature and Pressure Measurements

	Pressure	Temperature
Intake Manifold	Omega Eng. Inc	Omega Eng. Inc
Exhaust Manifold	Omega Eng. Inc	Tempral Inc.
Post Turbocharger	Omega Eng. Inc	Tempral Inc.
Pre Compressor	Omega Eng. Inc	Tempral Inc.

Thermocouples work by having two different wires at the same temperature and the two wires create a voltage at the joined end that can be related to temperature. K-type thermocouples use nickel and chromium or aluminum for the wire set. The thermocouple used in the intake manifold came from Omega Engineering (Stamford, Connecticut). It has a one eighth of an inch diameter, can measure temperatures up to 500°F (260°C), and has an error of 2.2°C. The other thermocouples came from Temprel Incorporated (Boyne, Michigan), model number T-26. It can measure temperatures up to 1650°F (900°C), with an error of 1.1°C. The strain gage pressure transducers use a strain gage that is distorted by exerted pressure due to force and relates that force to an electrical resistance. All four transducers came from Omega Engineering (Stamford, Connecticut). The PX309-050A5V transducer models have a pressure range from 0 to

3.45 bar with an error of 0.25%. Temperature and barometric pressure are measured at the air intake using temperature and pressure sensors from Omega Engineering.

2.2.2 Fuel Flow Rate

The fuel is pumped into a fuel cabinet designed and built by the AERL at Texas A&M University and this is also where it is measured. Fuel enters the cabinet and goes through three Max Machinery components which are shown in Figure 8.

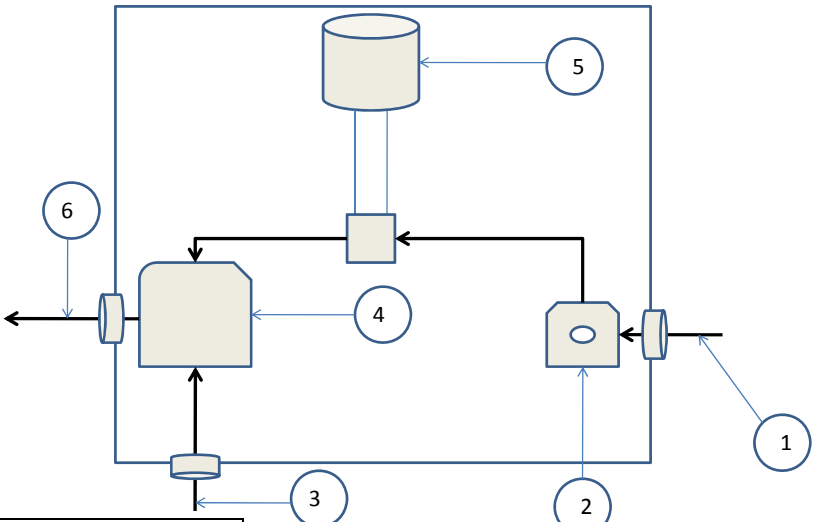

1	Fuel Supply Line
2	Vapor Eliminator
3	Engine Fuel Return
4	Fuel Level Controller
5	Signal Transmitter and Fuel Meter
6	Engine Fuel Supply

Figure 8: Fuel Cabinet Layout

The first is a vapor eliminator. It removes air vapor bubbles in the fuel supply line before the fuel gets to the fuel meter. It operates at a maximum pressure of 5.17 bar and depending on the fuel flow rate it can eliminate air at a rate of 300 to 2100 cubic

centimeters (cc) per minute. The vapor eliminator is followed by the fuel meter and the signal transmitter. The fuel meter has a flow rate range from 1 to 1800 cc per minute and an accuracy of 0.2%. The fuel meter is a piston type flow meter with four radial pistons which rotate around a central shaft. The fuel is pumped into a central cavity, where the pistons work together to pull fuel in and expel it out. Fuel is measured by the displacement of each piston. The crankshaft is connected to an electronic meter which measures flow in terms of a voltage output between 0 to 10 volts. This voltage signal is then sent to the data acquisition system. Once the fuel leaves the fuel meter it flows into the level controller. There are two main functions of the level controller; it has a supply tank that supplies fuel to the engine and it returns the bypass fuel from the common rail injection system back into the supply tank. The supply tank level is controlled by a mechanical float indicator which meters fuel used by the engine. The tank is equipped with avent system that keeps vapor or bubbles out of the fuel line. It has a flow rate of 1500 cc per minute for diesel and about 1000 cc per minute for pure biodiesel, with a maximum inlet pressure of 1.38 bar. The tank inside of the level controller has a maximum volume of 202 cc at 0.69 bar. All of the metering equipment can operate at a max temperature of 93.3 °C.

2.2.3 Emissions

Emission samples are pulled from the exhaust pipe through a heated filter and heated sample line that are kept at 190°C, and then it flows into a Horiba Emissions Bench. The bench is capable of measuring nitrogen monoxide (NO) through chemiluminescence. Chemiluminescence is light energy that is given off by a chemical

reaction; in this case the reaction is with ozone and NO. The CO_2 and CO concentrations are detected through non-dispersive inferred absorption, which detects the concentrations of the gas by optical absorption of that particular gas infrared wave length. O_2 concentrations are measured through a magneto pneumatic analyzer. A magneto pneumatic analyzer uses a nonhomogeneous magnetic field to create a pressure difference between a known gas concentration and the gas to be analyzed. This pressure difference is converted into an electrical signal related to the oxygen concentration in the analyzed gas.

2.2.4 Dynamometer

The engine is loaded using a direct current dynamometer produced by General Electric. It is capable of 110 kW of power absorption and uses a wheatstone bridge strain gauge that measures the force used to calculate the torque produced by the engine. The energy absorbed by the dynamometer is dissipated by a resistor bank. Loading on the engine is done by introducing an electric current into the dynamometer. This current gives the dynamometer resistance to spinning. The engine compensates by adding more fuel to increase the power. An increase in power helps the engine to overcome the resistance from the dynamometer and maintain a set speed on the engine controller. The load percentages are the percentage of the engine's power being used to turn the dynamometer.

2.3 Test Fuels

The two fuels that were tested in this experiment were an ultra low sulfur certification diesel (ULS) from Chevron Phillips Chemical located in The Woodlands, Texas, and a blended feed stock biodiesel (B100) from Organic Fuels in Houston, Texas. Both fuels are shown with their properties in Table 3. As seen in Table 3 the ULS diesel has a lower density and a higher heating value than the B100.

Table 3: Fuel Properties

Properties	***Diesel 2007 ULS***	***Blended Biodiesel Stock***
Density	**845 kg/m3**	**877 kg/m3**
Net. Heating Value	**42.89 MJ/kg**	**-**
Gross Heating Value	**45.11 MJ/kg**	**40.3 MJ/kg**
Cloud Point	**(-)27 FAH**	**-**
Flash Point	**152 FAH**	**-**
Pour Point	**(-) 9 FAH**	**-**
Sulfur	**8.2 ppm**	**-**
Viscosity	**2.1 cSt**	**-**
Cetane #	**44**	**-**
Particulate Matter	**.7 mg/L**	**-**
Hydrogen	**13.10%**	**-**
Carbon	**86.90%**	**-**
Aromatics	**29.1 LV%**	**-**
Polynuclear Aromatics	**7%**	**-**
SFC Aromatics	**31%**	**-**

2.4 Equivalence Ratio Calculation

The equivalence ratio calculation is based off of the emissions data. This method is good for both fuels that do and do not contain oxygen. The exhaust gas for this experiment was analyzed on a dry basis. The fuel is represented by $C_nH_mO_r$, where n, m, and r are the number of carbon, hydrogen, and oxygen atoms present in the fuel. The equivalence ratio is calculated using equation 1.

$$\Phi = \frac{(2 \times NO2)}{[Np \times (1 - XH20) \times (X*CO + 2 \times X*CO2 + 2 \times X*O2 + X*NO) - r]} \quad \ldots\ldots\ldots\ldots (1)$$

Where NO2 is the amount of oxygen needed for complete combustion to take place. Np is the total amount of moles in the exhaust products, and is calculated by equation 2.

$$Np = \frac{n}{XCO + XCO2} \quad \ldots\ldots\ldots\ldots (2)$$

The mole fraction of water was calculated using equation 3, and equation 4 was used to go between wet and dry mole basis.

$$XH2O = \frac{m}{2n} \times \frac{X*CO + X*CO2}{[1 + \left(\frac{X*CO}{K \times X*CO2}\right) + \frac{m}{2n} \times (X*CO + X*CO2)]} \quad \ldots\ldots\ldots\ldots (3)$$

$$Xi = (1-XH2O) \times X^{*}i \quad \ldots\ldots\ldots\ldots (4)$$

Xi is the wet mole basis and $X^{*}i$ is the dry mole basis. K is a constant and was 3.8 for this test, Stivender found that K has little if any affect on phi and that 3.8 was the best for engine exhaust products [9].

2.5 EGR Mass Fraction Calculation

The EGR mass fraction was calculated from the different species of gases in the intake. Each mole fraction of individual gases were multiplied by its molecular weight, then dived by the molecular weight of EGR to obtain the mass fraction of that species in EGR. Then all the individual mass fractions were summed to obtain the mass fraction of EGR in the intake. This is demonstrated by equations 5 and 6, where X_i and Y_i denote mole and mass fractions.

$$\frac{X_i \times M_{mw}i}{M_{EGR}} = Y_i \quad (5)$$

$$Y_{EGR} = \sum Y_i \quad (6)$$

The uncertainty calculated for the EGR mass fraction and the dilution ratio was calculated using an error propagation method [10]. This method is good for calculating the uncertainty of a value (R) when it has two or more independent variable that add their own uncertainty to R. Equations 7, 8, 9, and 10 shows how the uncertainty is calculated using the error propagation.

$$\delta R_{i+} = R_i + U_i \quad (7)$$

$$\delta R_{i-} = R_i - U_i \quad (8)$$

$$\delta R_i = \frac{\delta R_{i+} + \delta R_{i-}}{2} \quad (9)$$

$$U_R = \pm\left[\sum\left[\delta R_i\right]^2\right]^{\frac{1}{2}} \quad (10)$$

2.6 Data Collection

A nine point test matrix was conducted holding the speed constant at three different speed settings (1400, 1900, and 2400 rpm). Then each speed was tested at three different loads (20, 60, and 75%) as shown in Table 4.

Table 4: Nine Point Test Matrix

Load	Speed (rev/min)
20%	1400
	1900
	2400
60%	1400
	1900
	2400
75%	1400
	1900
	2400

The engine was held at each test point for about 20 minutes and the coolant temperature was recorded to ensure there was no fluctuation occurring in the engine before the data was recorded. The data was digitally recorded by LabVIEW, and processed using Microsoft Excel. There are 300 averaged data points recorded at each test point in the matrix and each test matrix will be repeated four times for each fuel. The four data sets from the experiment were averaged and analyzed in Excel and graphed using Tecplot 360. Air flow and air to fuel ratios were calculated using a method by Heywood

[11]. The results for the emissions, temperatures, air flow, and air to fuel ratio from the two fuels were compared and analyzed.

3 RESULTS AND DISCUSSION

3.1 Characteristics

To get an idea of how the engine behaves the test matrix was first operated with the ULS diesel. This was done so that the lab would always have a base line comparison to go back to if there was ever any concern about any data that was taken. The factory settings could be restored and any deviations could be analyzed against this data. Then the tests were run with the ULS and the B100 to compare the effect of the two fuels on the engine's exhaust species.

This section will focus on the characteristics of the engine. These characteristics will focus on describing how the engine behaves at different loads and speeds. The parameters that will be discussed are torque, fuel flow rate, air flow rate, air-fuel ratio, CO, O_2, CO_2, EGR, and NO.

One main characteristic of an engine is the torque curve. An ideal torque curve would start out at maximum torque and at the lowest speed. The torque would stay constant throughout the range of speeds of the engine. Effects such as heat transfer and friction, however, causes deviations between the actual torque curve and the ideal torque curve as the engine speed varies. Even though the speed of the engine does not have a direct effect on torque, it does on heat transfer, friction, and volumetric efficiency. At low speeds a greater fraction of fuel energy is lost to heat transfer due to the longer period of time it takes heat transfer to occur. As engine speed increases, the decreased

time for heat transfer hinders its effect. Fuel energy lost to friction increases with squared engine speed. The same effect is seen with the volumetric efficiency as engine speeds increases. Volumetric efficiency is the volume of air taken into the cylinder divided by the ideal volume the cylinder displaces. Ideally an engine should burn the maximum amount of fuel and air that the displaced volume will allow achieving maximum power production. Normal valve timing, however, only allows for a certain speed range at which this is possible. As a result of these valve characteristics (timing, lift, geometry, and size), intake and exhaust manifolds are designed to allow for maximum volumetric efficiency at a certain engine speed. For this engine that speed is 1400 rpm, as seen in Figure 9.

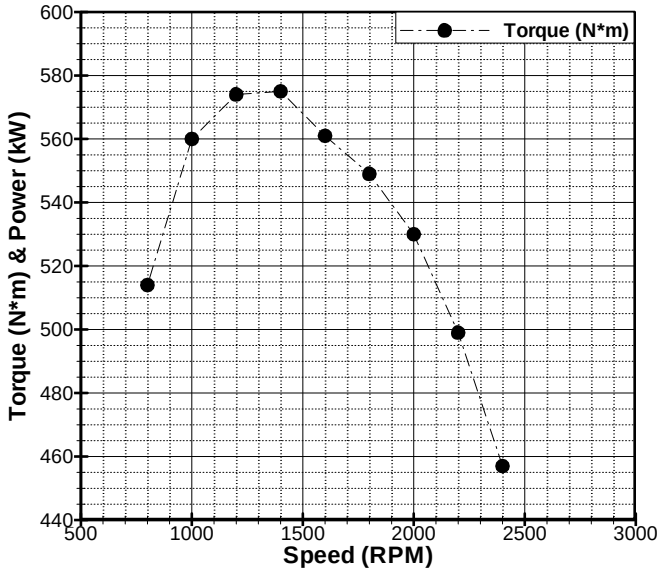

Figure 9: Torque vs. Speed: Full Load

In Figure 9, 1400 rpm is where the maximum torque is achieved. If the volumetric efficiency curve were plotted over the power curve, the two would have almost identical shapes, with the highest volumetric efficiency occurring around the same speed. Any speed before or after 1400 rpm has a lower volumetric efficiency, as a result of the valve timing causing the piston to push out some of the charge of air before the valve closes and the exhaust valve trapping the exhaust gases in the cylinder diluting the incoming charge. Friction, heat transfer, and volumetric efficiency are the major reasons why the actual torque curve is not a constant line at the maximum torque value. Friction and heat transfer are the reasons why the engine does not convert all of the fuel energy into useful energy. The next set of data will be used to characterize the engine. Figure 10 shows the torque versus speed graph for the petroleum diesel at three different loads. As seen in Figure 10 the torque peak is at a mid speed; this is because the engine is only at partial load and not full load. There is about 13 Newton-meter (N·m) difference in the average between 1400 and 1900 rpm at 75 percent load.

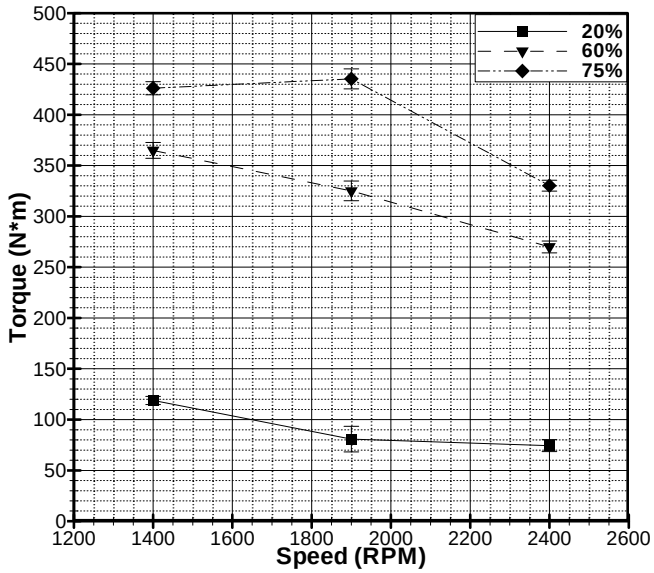

Figure 10: Torque vs. Speed of ULS Diesel

The torque rises as the load increases, but falls as the speed increases, with the only exception at 75 percent load going from 1400 rpm to 1900 rpm. Even though Figure 2 is not showing maximum torque it still has the same limiting factors acting upon each load condition as the maximum load curve does. These factors may have different effects at loads less than the maximum, which would be why there is a rise in torque after 1400 rpm for 75 percent load. At full load the engine produces about 400 lb*ft of torque at 1900 rpm; however each load produces the lowest torque at 2400 rpm. This is due to the overwhelming frictional forces acting on the engine at the higher speeds. The uncertainty bars at each point show the two sigma (95%) confidence range for each measurement, proving that high reproducibility was achieved over several days of testing.

Figure 11 shows the fuel flow rate. This will give some insight on how well the engine converts fuel energy into useful energy, and how much fuel the engine uses at certain speeds and loads. The fuel flow rate for the three test conditions are displayed in Figure 11. Corresponding to Figure 10 as the load increases the amount of fuel increases.

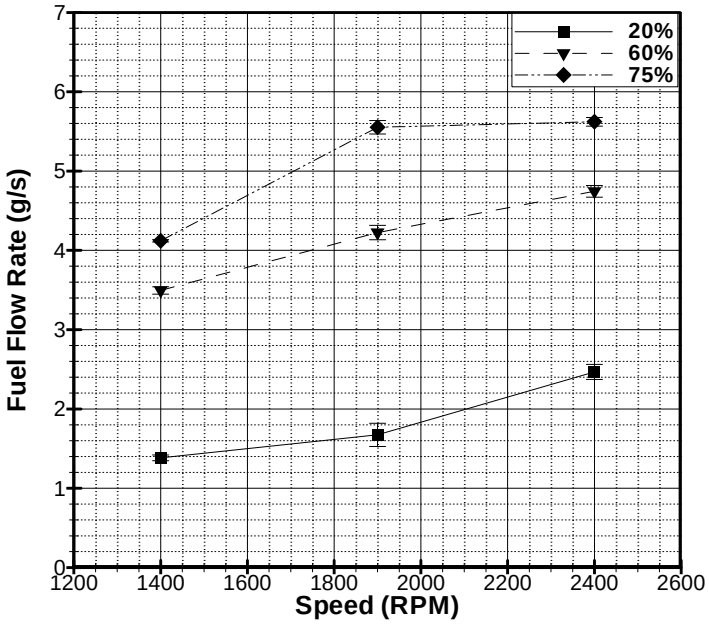

Figure 11: Fuel Flow Rate vs. Speed of ULS Diesel

The engine uses more fuel with increase in speed and load. At high loads and speeds more fuel is needed, but does not mean that more torque is produced as the engine speed increases. Similarly to Figure 10, Figure 11 also displays an acceptable uncertainty for each measurement.

Before the emissions can be characterized the air flow should be looked at since the air-fuel ratio is calculated from the fuel flow and air flow rates, and not measured. Figure 13 shows the air flow rate for all three speeds and loads.

However, there was an error found in the air flow rate measurement that is currently being worked out. This error caused the air flow rates to vary between 10 to 30%. In order to correct the problem the air-fuel ratio has been calculated three ways using the emissions data collected from the emission bench. The emission bench was calibrated with calibration gases before each and every data set taken to ensure that the analyzers were reading correctly. The three ways to calculate the air-fuel ratio are one based on a carbon balance, oxygen balance, and an equivalence ratio based on dry gas analysis [11]. The air fuel ratio was calculated using the stoichiometric air fuel ratio. After the equivalence ratio was calculated the air flow rate was calculated using the air-fuel ratio and the fuel flow rate measurement. Figure 12 shows the air-fuel ratio of all four calculations.

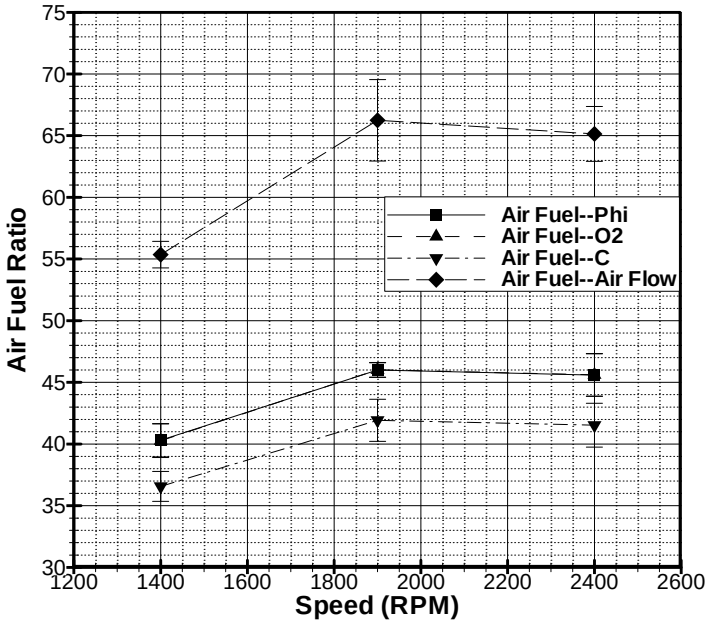

Figure 12: Air-Fuel Ratio Comparison of ULS Diesel

The air-fuel ratio determined by the equivalence ratio and oxygen balance lay right on top of each other, while the carbon based air-fuel ratio gives values just under the equivalence ratio, and oxygen balance. The air-fuel ratio based on the air flow rate is very high compared to the other three, because of the erroneous air flow rate. All four plots do follow the same pattern, rising at the mid speed and slightly falling at the high speed.

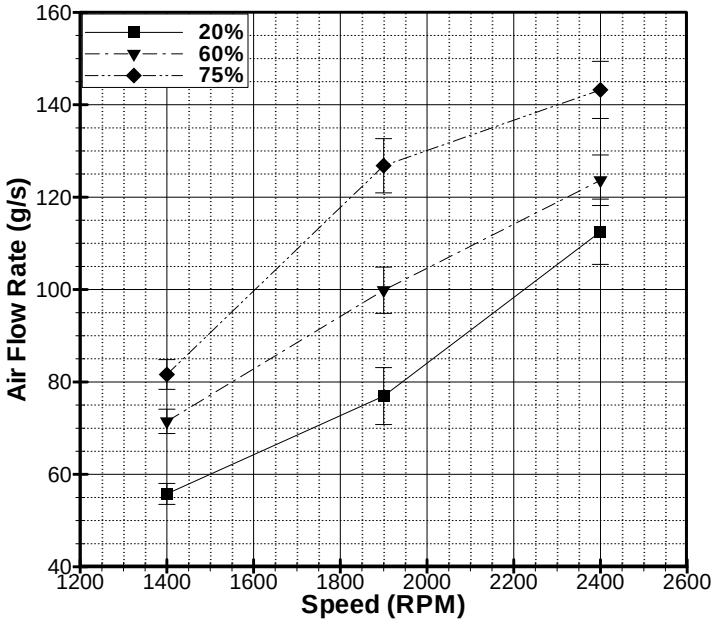

Figure 13: Air Flow Rate vs. Speed of ULS Diesel

The engine takes in more air as the speed increases. A load of 75 percent load flows the most air at all speeds. The amount of air taken in by the engine is different at all speeds and loads (except at 2400 rpm at 20 and 60 percent loads, where there is not 95% confidence that the data is different). The air flow rate and fuel flow rate do not increase at the same proportion regardless of speed or load. More air is being taken in than fuel; this is why the engine runs leaner as the speed increases and is reflected in Figure 14.

Figure 14 displays the air to fuel ratio with respect to engine speed and load. Before emissions can be analyzed the air-fuel ratio must be taken into consideration first, because it directly affects O_2 and CO_2 emission. This effect will be shown in Figure 15 and Figure 16.

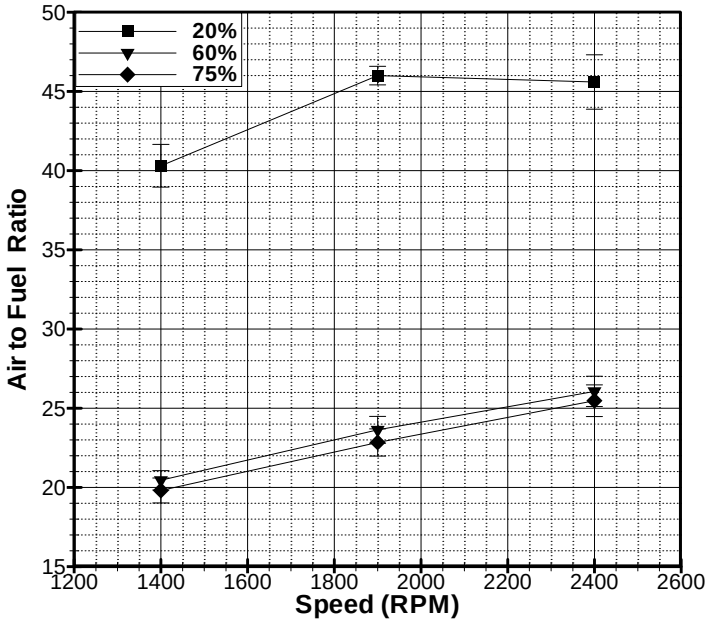

Figure 14: Air-Fuel Ratio vs. Speed of ULS Diesel

Overall the engine runs the leanest at low loads and high speeds, and the lowest air to fuel ratio occurs at the highest load and the lowest speeds. This occurs because as more of a load is placed on the engine more fuel and air are needed to supply the needed power. Since the air fuel ratio is defined as the mass of air over the mass of fuel the ratio will continue to rise as the mass of air increases faster than the mass of fuel. Why is this important to the O_2 and CO_2 emissions? Equations (1) and (2) show combustion of diesel with air-fuel ratios of 14.3 and 28.3 (mass basis), respectively. The effect of the air-fuel ratio on molar concentration of the combustion products is apparent in the equations.

$C_{14.4}H_{24.9} + 20.625*(O_2 + 3.76 * N_2) = 14.4*CO_2 + 12.45*H_2O + 20.625*(3.76*N_2)$. . . . . .(11)

$2*C_{14.4}H_{24.9} + 82.43*(O_2 + 3.76*N_2) = 28.8*CO_2 + 24.9*H_2O + 82.43*(3.76*N_2) + 41.18*O_2$. . . . . .(12)

From these two equations obviously there is enough O_2 for combustion to take place, and as more air than fuel is added more O_2 is emitted, which explains the O_2 emissions in Figure 15.

3.1.1 Emission Characteristics

Today, emissions are major criteria in engine design. Every year emissions for both spark ignition (SI) and compression ignition (CI) engines are more and more stringent. This section will focus on characterizing the emission behavior of the engine under the different loads and speeds. An ideal engine combustion process would only yield CO_2, H_2O, O_2, and nitrogen, but actual combustion yields those products along with NO, CO, hydro carbons (HC), and several other trace constituents.

The emissions characterization will start out displaying O_2 followed by CO_2, CO, and NO concentrations. The O_2 concentrations are displayed in Figure 15.

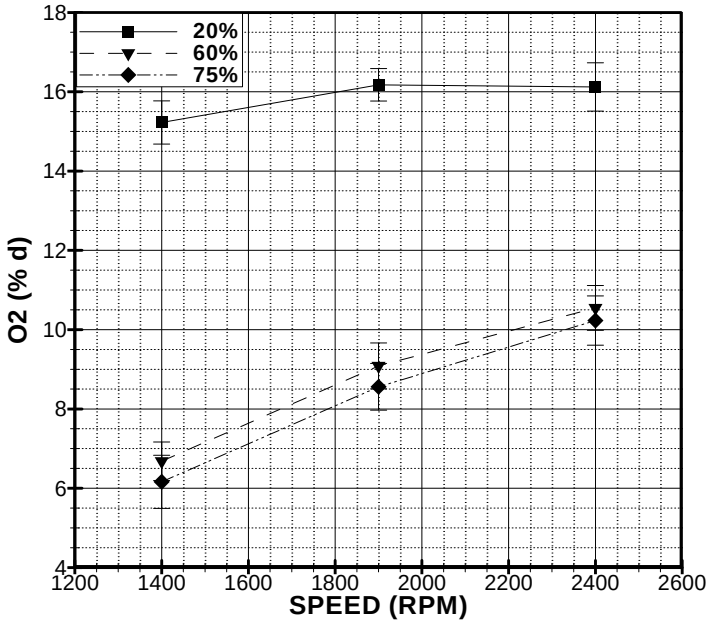

Figure 15: O_2 vs. Speed of ULS Diesel (% d-molar percentage on a dry basis)

In Figure 15, as the load increase the O_2 concentration decreases, but the percentage of O_2 increases as the speed increases. This figure correlates with Figure 14 identically, which shows the air-fuel ratio. All the fuel is burned leaving the excess O_2 to emit out into the exhaust, the leaner the engine runs the more oxygen is emitted into the exhaust. This affects the data shown in Figure 16, which shows CO_2 decreasing as speed increases.

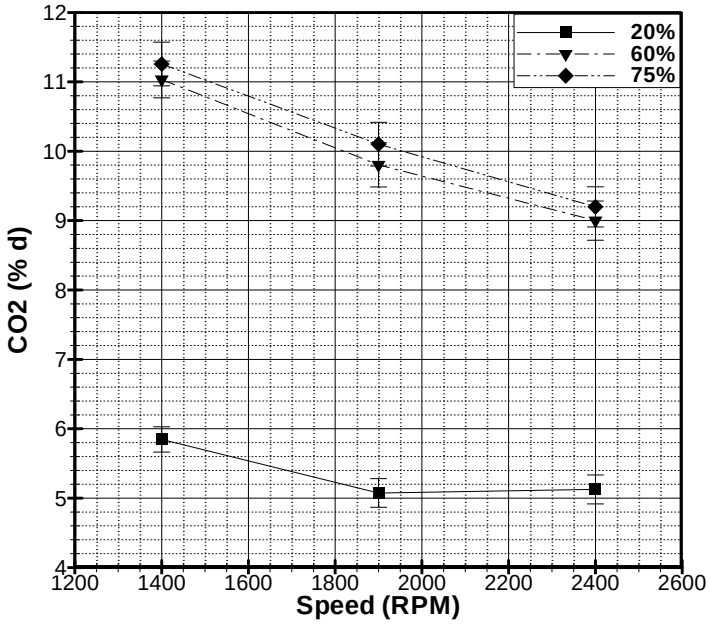

Figure 16: CO_2 vs. Speed of ULS Diesel

CO_2 characteristics of the engine are displayed in Figure 16. The data in this figure are the opposite of that shown in Figure 14. CO_2 concentrations rise with the increase in load because the fuel is increased, but decrease as the speed increases with each load. The decrease with speed is the opposite of what is exspected since the engine takes in more fuel as speed increases. By looking at Figure 14 and Figure 15 the O_2 increases along with the air-fuel ratio, meaning that the amount of air and fuel are both increased, but more air than fuel. As more fuel is burned there are more hydrocarbons, more hydrocarbons plus more air, should equal more CO_2 in the exhaust. The reason this is not shown in Figure 16 is shown back in Equations 1 and 2. So of course the more fuel burned the more carbon dioxide is produced, but the molar concentration goes down because of the additional amount of O_2 coming out of the cylinders. The CO_2

Molar percentages of CO_2 decrease in equation 2 compared to 1, but there are more moles CO_2 as moles of fuel increase. Mole percentage of CO_2 went from 13.8 percent to 7.1 percent as more air is taken in and the extra oxygen shows up in the products. This is why there appears to be less CO_2 in the exhaust as the engine speeds up.

Diesel engines run lean and for this reason CO and unburned hydrocarbon concentrations are not a major issue. Figure 17 is a prime example of low CO concentrations from diesel engines.

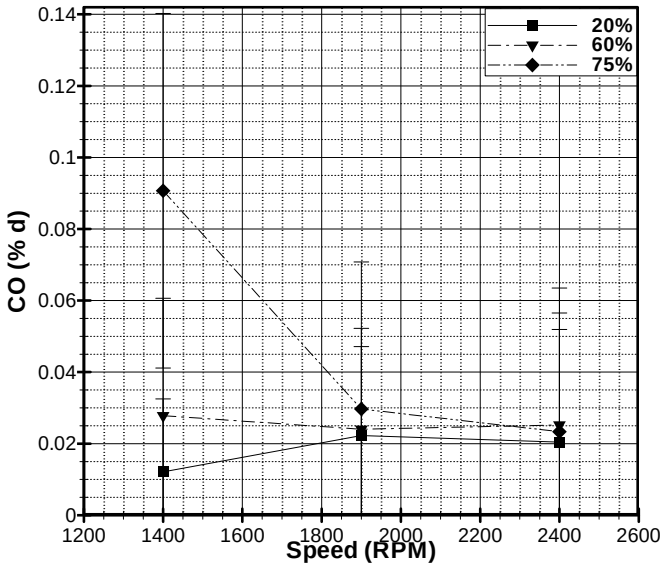

Figure 17: CO vs. Speed of ULS Diesel

In Figure 17 the CO concentrations are displayed. The CO is very low at all loads and speeds. All conditions are around 0.05 percent with the exception of the 1400 rpm, 75 percent load case. It is double the amount of the other data points. CO concentrations are low for diesel engines in general because of the lean running

conditions. The lean or oxygen rich running condition of diesel engines allow for the CO present in the exhaust to oxidize in to CO_2 as seen in complete combustion. There is a very high uncertainty here because of the low concentration of CO being emitted into the exhaust are close to the lower limits of the analyzers.

One of the most important emissions characteristic of any internal combustion engine of today would be NO emissions. Diesel engines have high NO emission due to the high compression ratios, which have high in-cylinder pressures and temperatures. NO_x thrives under these conditions. The highest NO emissions occur when the equivalence ratio (is the stoichiometreic air-fuel divided by the actual air-fuel ratio) is around 0.85 to 1.1 [11]. During combustion NO is formed at high temperatures by nitrogen bonding with the free oxygen in the cylinder. One way to control or minimize NO is to dilute the in-cylinder charge making combustion happen at lower temperatures; today this is done with EGR. This next set of data will show how the engine behaves with EGR and how it affects NO concentrations. Figure 18 shows the dilution ratio for all speeds and loads. The dilution ration is the ratio of carbon dioxide in the intake manifold divided by the carbon dioxide in the exhaust. The dilution ratio along with the exhaust products were used to calculate the amount of EGR in the intake manifold shown in Figure 19. First the dilution ratio was used to calculate the amount of water, CO_2, CO, O_2, and N_2 present in the intake. Then the mass fraction of EGR of each species was calculated and added together to calculate the total mass fraction of EGR in Figure 19.

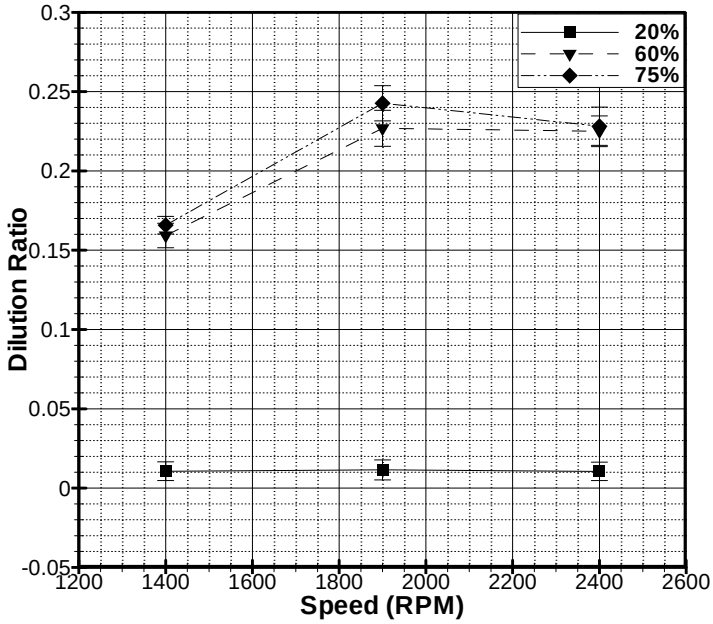

Figure 18: Dilution Ratio vs. Speed of ULS Diesel

At low loads there is hardly any CO_2 present in the intake manifold. Carbon dioxide starts to present itself during the mid and high load conditions. This is when the engine is flowing EGR. Both the mid and high load condition have the same pattern, the dilution ratio rises at 1900 rpm and has a slight drop at 2400 rpm. The high load condition has a higher average, but there is no statistical difference between the mid or high load conditions.

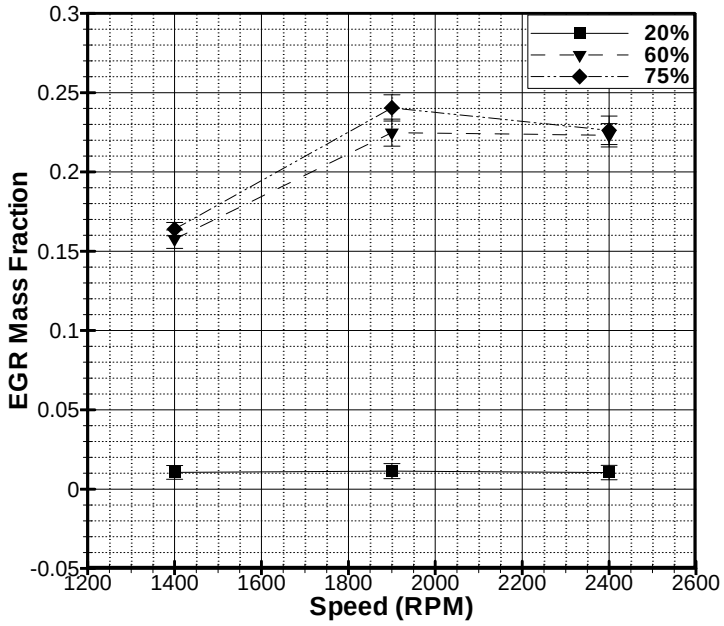

Figure 19: EGR Mass Fraction in the Intake Manifold vs. Speed of ULS Diesel

At low loads the engine does not flow any EGR. EGR flows during the mid to high load ranges. The amount of EGR peaks at 1900 rpm for both the mid and high load condition. The EGR is controlled specifically by the engine's ECU (engine control unit), and it is pre-programmed by John Deere. The ECU starts the flow of EGR when the coolant temperature reaches 170 degrees Fahrenheit and above, any temperature below 170 the EGR flow stops. The NO concentrations were corrected for humidity using SAE J1243 for emissions corrections, because the lab is subject to open air conditions [12]. Figure 20 displays the corrected NO concentrations in ppm (parts per million).

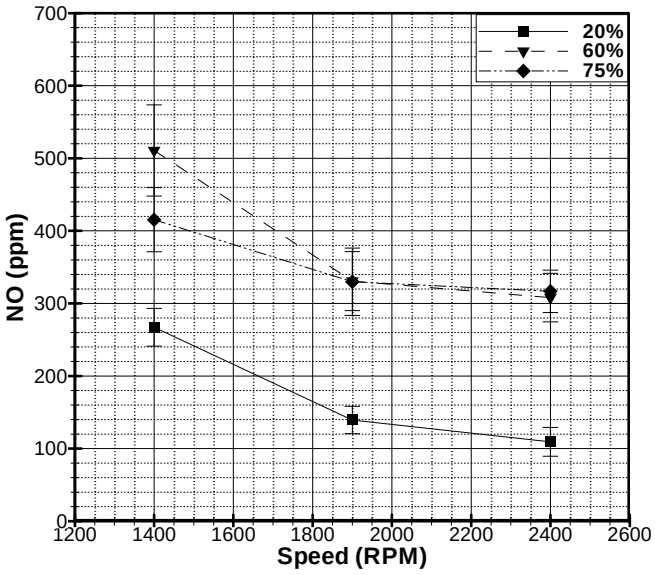

Figure 20: NO vs. Speed of ULS Diesel

Figure 20 shows the NO concentrations characteristics for the three speeds and loads. A similar trend is found at all load conditions, which is that the NO concentrations decrease as engine speed rises. Speed along with EGR is involved in how the NOx emissions are affected, as heat transfer has less of an effect at high speeds and the EGR dilutes the intake charge cause lower flame temperatures during combustion [13]. At higher speeds there is less time for heat to transfer to the exhaust gases not giving the NO reaction the energy it needed to take place, which freezes the reaction in the exhaust. The mid load condition has the highest amount of NO concentrations at 1400 rpm, and then they are the same for the 1900 and 2400 rpm as the 75 percent load. The 20 percent load has the least amount of NO concentrations at all speeds, and this is without EGR. This is because of the temperature and pressures are not as high as the mid and high load conditions

Now that the engine's emissions have been characterized the ULS diesel will be compared against the B100 in order to see how well the B100 is suited for a diesel replacement.

3.2 Biodiesel Versus ULS Reference Diesel

3.2.1 Characteristics Comparison

The ULS and Biodiesel torque curves will be compared to see if the B100 will be an adequate replacement for petroleum diesel. Figure 21, Figure 22, and Figure 23 show the torque comparisons for the different loads and speeds.

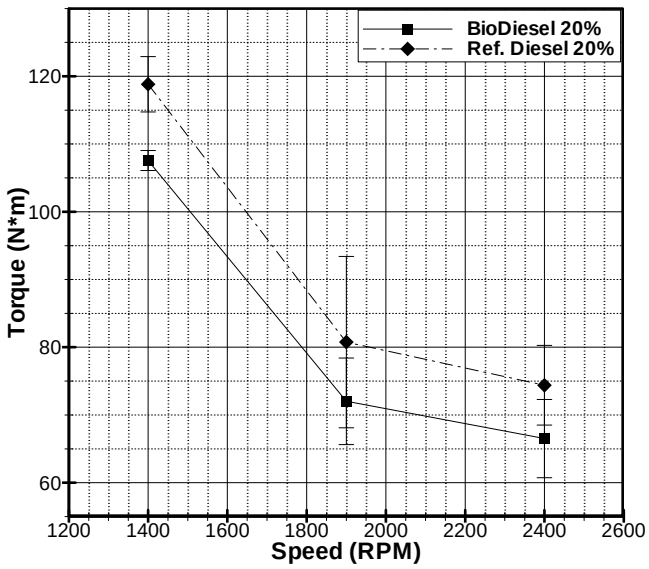

Figure 21: Torque at 20% Load vs. Speed

The torque curves for 20 percent load in Figure 21 follow the same pattern. As the speed rises the torque falls for both fuels. The B100 averages less torque at all three

speeds, but there is not a statistical difference with in a 95% confidence range at 1900 rpm.

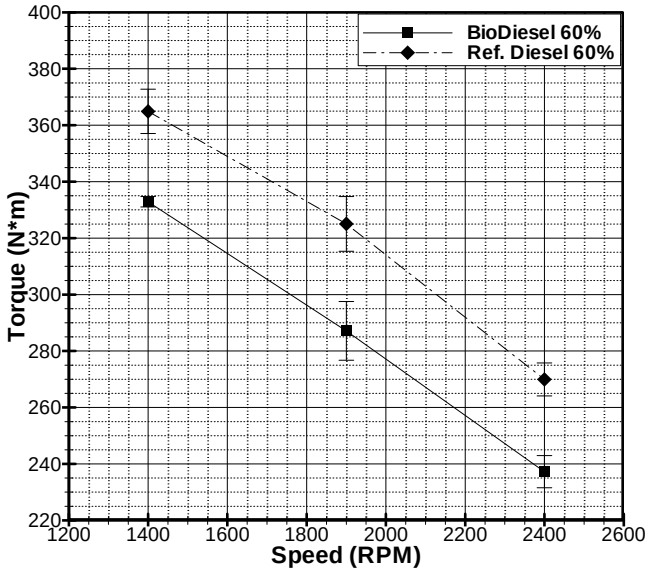

Figure 22: Torque at 60% Load vs. Speed

Like Figure 21, Figure 22 also shows B100 producing lower torque values at all speeds, however the differences in the two fuels torque production is of greater magnitude. Again Figure 23 shows the B100 producing less torque at all speeds, however with the biggest difference being at 1900 rpm.

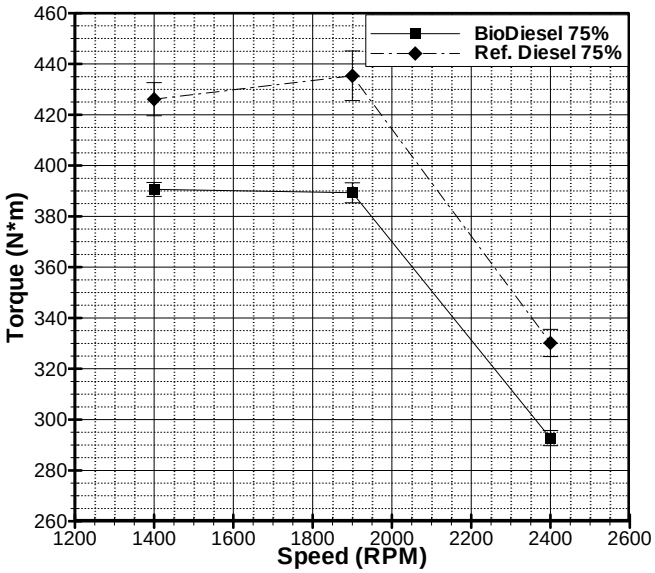

Figure 23: Torque at 75% Load vs. Speed

The trends in the previous three figures can be attributed to the same reason as in Figure 9, and those reasons are heat transfer, friction and volumetric efficiency. However the reason why the ULS produces more torque than the B100 at all speeds and loads can be attributed to B100 having a lower heating value (ULS higher heating value is 45.11MJ/Kg and B100 higher heating value is 40.3 MJ/Kg as previously shown in Table 3). This statement is further proven by Figure 24 through Figure 26. Other factors such as combustion timing and burn duration may also cause the lower torque values. The combustion timing depends heavily on the injection timing, and biodiesel is known for having earlier injection timing than petroleum diesel. The earlier injection timing would cause an early combustion timing, which if happens too soon or too late would cause a drop in peak pressure and temperature and thus a loss of torque production. One way to tell if the heating value of the fuels is the cause for the

difference in the torque production would be to look at the fuel flow rates at each speed in Figure 24, Figure 25, and Figure 26.

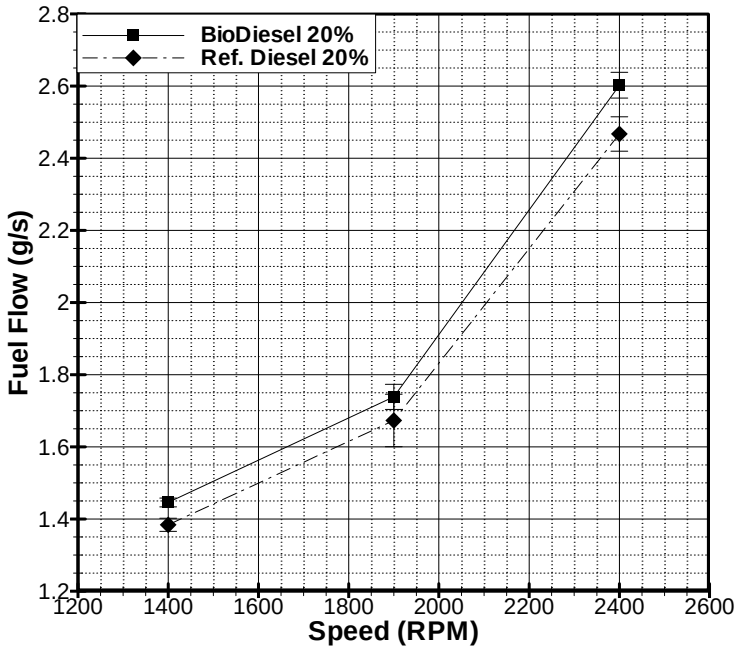

Figure 24: Fuel Flow Rate at 20% Load vs. Speed

Figure 24 has the fuel flow rate plotted for the 20 percent load condition for both fuels. The fuel flow rate increases as the speed increases, and the engine consumes more of the B100 at every speed. Figure 25 shows the 60 percent load fuel flow rate.

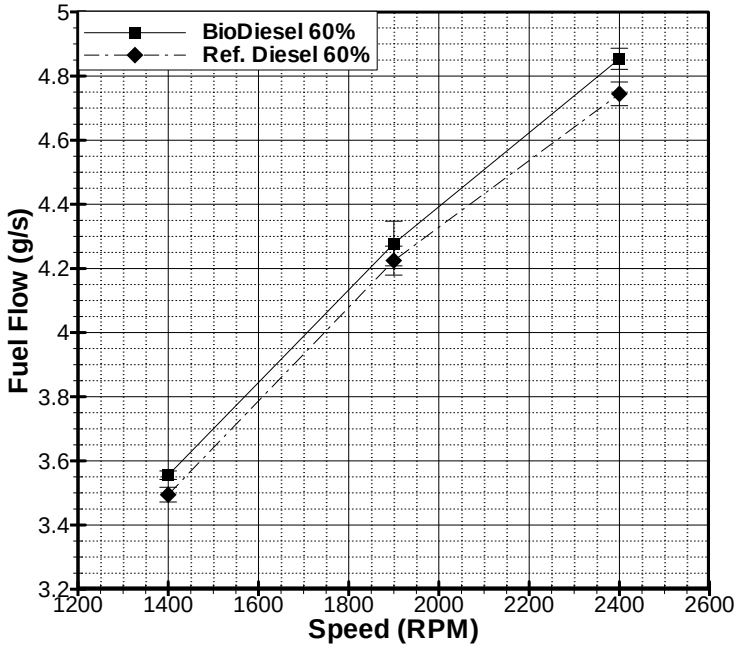

Figure 25: Fuel Flow Rate at 60% Load vs. Speed

The higher load causes for higher fuel flow rates in Figure 25 than Figure 24. As the speed increases the fuel flow rate increases just like Figure 24, and again the B100 has a higher fuel flow rate. The last fuel flow rate is shown in Figure 26 which displays the 75 percent load condition.

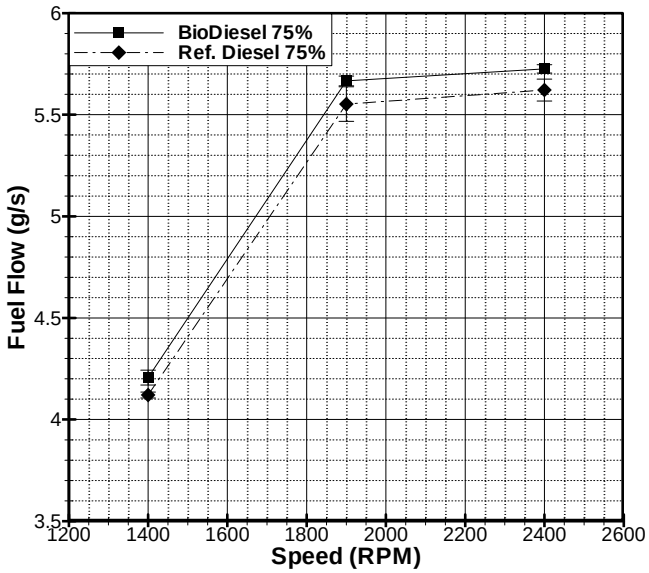

Figure 26: Fuel Flow Rate at 75% Load vs. Speed

In Figure 24, Figure 25, and Figure 26 the fuel flow rate for both fuels are displayed for all three loads at all speeds. The fuel flow rate goes up along with the speed and load for all three figures. The B100 has a higher flow rate in all three load conditions, and Figure 21 through Figure 23 the B100 produced less torque at all test points. So in order to get the engine to produce the same amount of torque even more B100 will be need at each speed.

Both the equivalence ratio and the air flow rate are calculated measurements from the emissions data collected by the engine. The equivalence ratio is the stoichiometric air- fuel ratio divided by the actual air-fuel ratio. The equivalence ratio will give more insight to why the emissions behave differently between the two fuels. Since the actual air-fuel ratios would be similar because of the closeness of the fuel flow rate and the air flow rates (which will be shown next). This would give the illusion that

the fuels have similar chemical formulas, and just looking at the actual air-fuel ratio there would be no way to tell how much leaner or richer one fuel burned from the other. Since the equivalence ratio uses both the actual air-fuel ratio and stoichiomtetric it will show the differences in how the fuel burns. The equivalence ratio is rich for any values greater than one and lean for values less than one. In order to calculate the actual air-fuel ratio to use in the equivalence ratio the air flow rate was measured in order to calculate the actual air-fuel ratio. Figure 27, Figure 28 and Figure 29 show the air flow for both fuels for all speeds and loads.

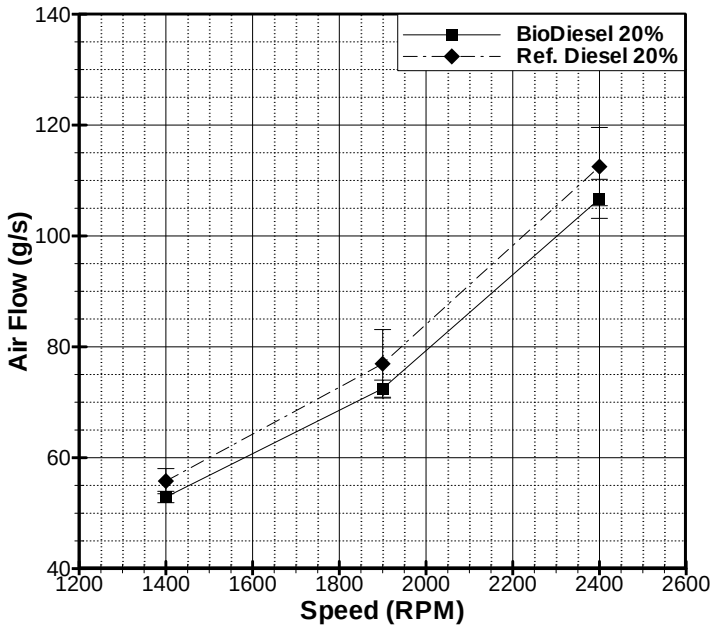

Figure 27: Air Flow Rate at 20% Load vs. Speed

In Figure 27 the air flow averages for the ULS is higher at all speeds than the B100, but there is only a statistical difference at 2400 rpm. Air flow increases along with the speed.

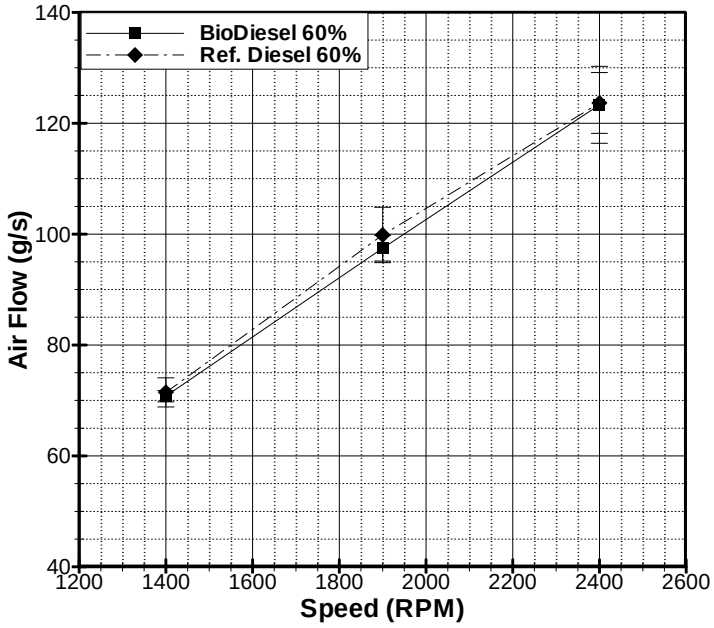

Figure 28: Air Flow Rate at 60% Load vs. Speed

Similar to Figure 27 in Figure 28 the same pattern is displayed at 60 percent load, unlike Figure 27 there is almost no difference in the averages of the two fuels.

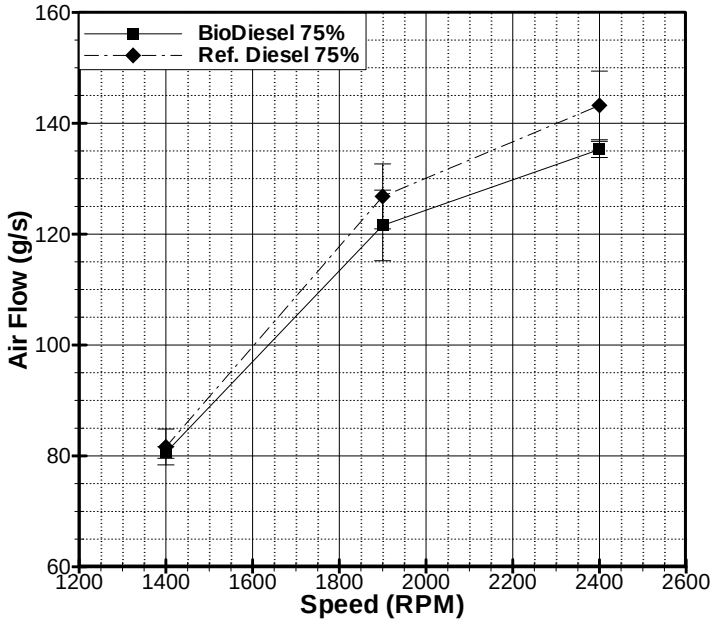

Figure 29: Air Flow Rate at 75% Load vs. Speed

Figure 29 displays the air flow rate at 75 percent load. The two fuels again as in the previous two figures show essentially the same air flow rate until 2400 rpm, also the air flow increases along with the speed.

The engine flows virtually the same air flow rate for both fuels except at high engine speeds and loads. Now that the fuel flow rate and the air flow rate has been measured the actual air-fuel ratio will be used to calculate the equivalence ratio. The actual air-fuel ratio on a mass basis was calculated for the ULS using Equation 3 which uses the empirical chemical formula of ULS.

$$CH_{1.8} + 1.45*(O_2 + 3.76 * N_2) = CO_2 + 0.9*H_2O + 1.45*(3.76*N_2). \quad (13)$$

Equation 3 yielded the stoichiometric air-fuel ratio to be 14.42 on a mass basis. The stoichiometric air-fuel ratio for the B100 was 12.6, which was found for 100 percent

Rapeseed Methyl Ester [5]; Kinoshita, et al [14]. also found similar air-fuel ratios. Figure 30, Figure 31, and Figure 32 will display the equivalence ratios for all three loads.

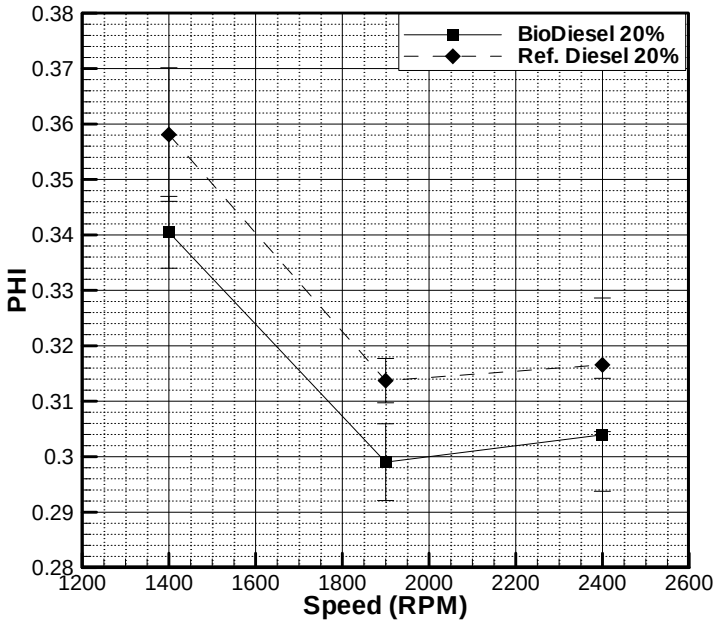

Figure 30: Equivalence Ratio at 20% Load vs. Speed

The equivalence ratio in Figure 30 shows that the ULS burns richer than the B100 at all speeds at 20 percent, except at 2400 rpm, the average is higher but the ULS has no statistical difference.

Both fuels follow the same pattern of getting leaner going from low to mid speed, and then slightly rising at the high speed condition, which correlates with the sharp increase in fuel flow rate in Figure 24: Fuel Flow Rate at 20% Load vs. Speed.

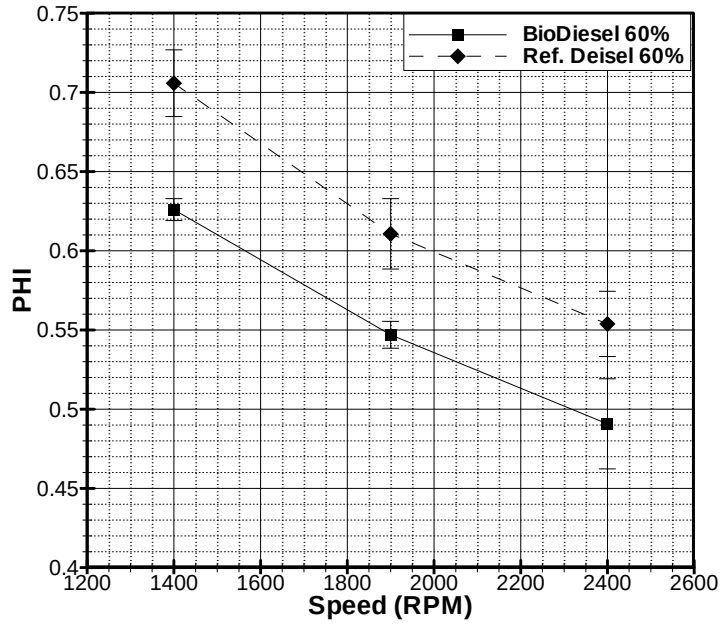

Figure 31: Equivalence Ratio at 60% Load vs. Speed

In Figure 31 the differences between the two equivalence ratios is increased, with the ULS still running richer than the B100. Unlike Figure 30 the fuels burn leaner as the speed increases, and the same pattern follows into the 75 percent test condition in Figure 32.

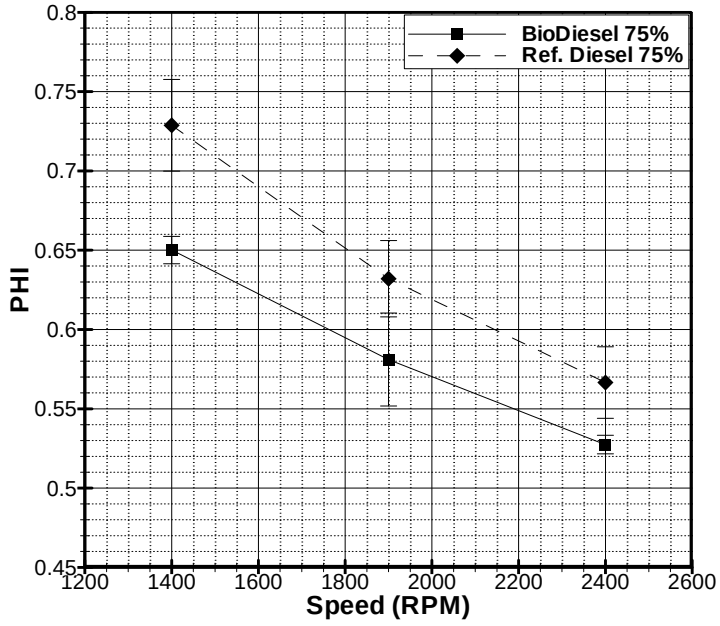

Figure 32: Equivalence Ratio at 75% Load vs. Speed

As the load increases, so does the fuel content as expected, thus the reason why the engine runs richer as load increases. B100 runs leaner than the ULS at all speed and load conditions, one reason for this can be attributed to biodiesel having an O_2 content of 11 percent, while the ULS has none [3, 15]. This would also explain why B100 emits more O_2 in Figure 33, Figure 34, and Figure 35, and as the engine is loaded the air intake increases for both fuels, therefore more O_2 is present in the exhaust.

3.2.2 Biodiesel vs. ULS Diesel Emissions

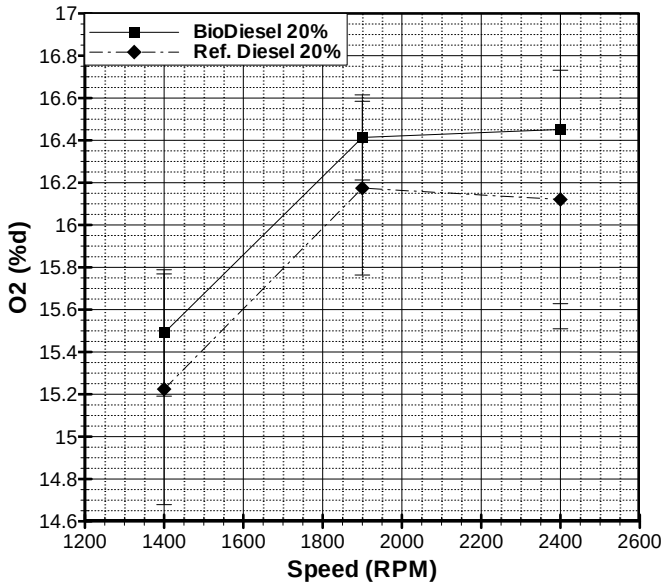

Figure 33: O_2 at 20% Load vs. Speed

B100 has higher averages of O_2 but there is statistical difference in the exhaust at 20 percent load at all speeds as seen in Figure 33. The oxygen content rises as the speed rises except for the last test condition of the ULS, where the O_2 concentrations fall from below those at 1900 rpm.

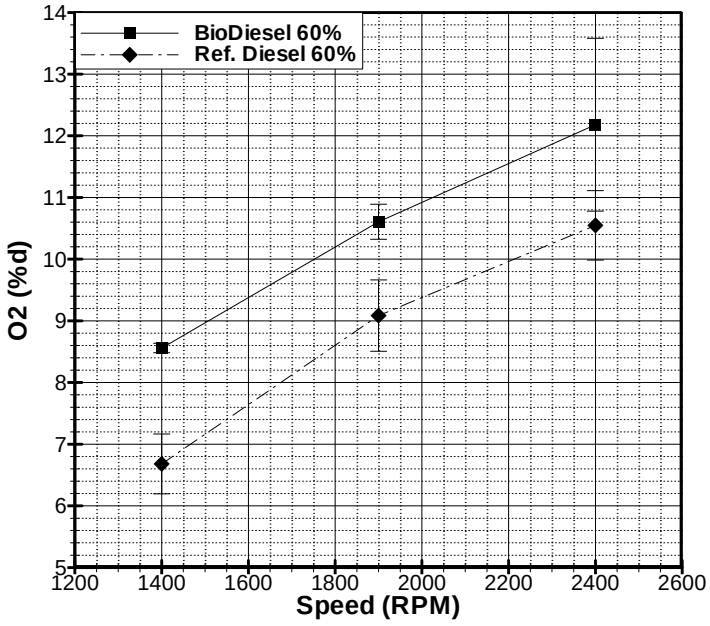

Figure 34: O_2 at 60% Load vs. Speed

Figure 34 shows the O_2 percentages at 60 percent load. The O_2 percentage for both fuels rise along with speed, and the ULS emits O_2 at all speeds. In Figure 35 the same pattern taking place as in Figure 34. The concentrations rise as the speed rises, and B100 has the highest O_2 present in the exhaust at all speeds.

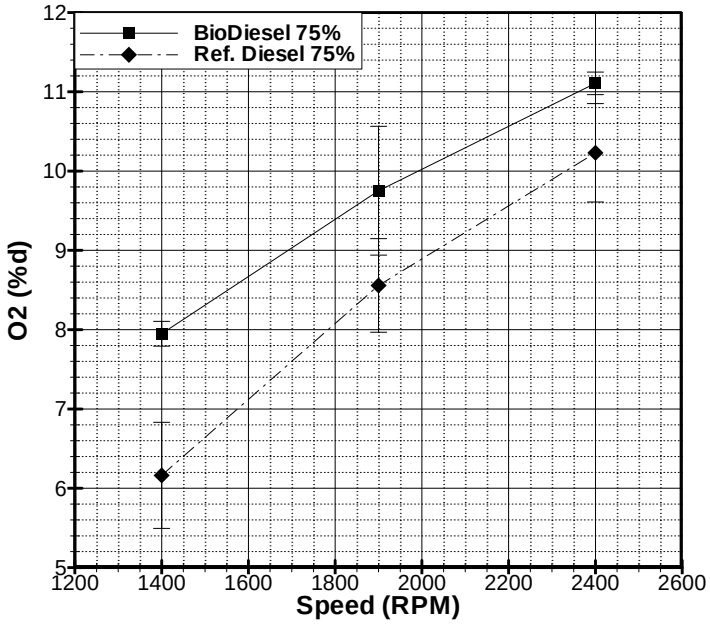

Figure 35: O_2 at 75% Load vs. Speed

The excess O_2 from the B100 also helps explain why it has a lower CO_2 concentration. As in the characterization with the ULS as the engine takes in more air than fuel the CO_2 molar concentrations will go down because there is more O_2 present in the exhaust. In the case for the B100 more O_2 is being brought in along with the O_2 already present in the fuel. Next the CO_2 will be compare since the O_2 concentrations directly affect the molar concentrations of the CO_2. Figure 36, Figure 37, and Figure 38 show the CO_2 concentrations for 20, 60, and 75 percent load conditions at 1400, 1900, and 2400 rpm.

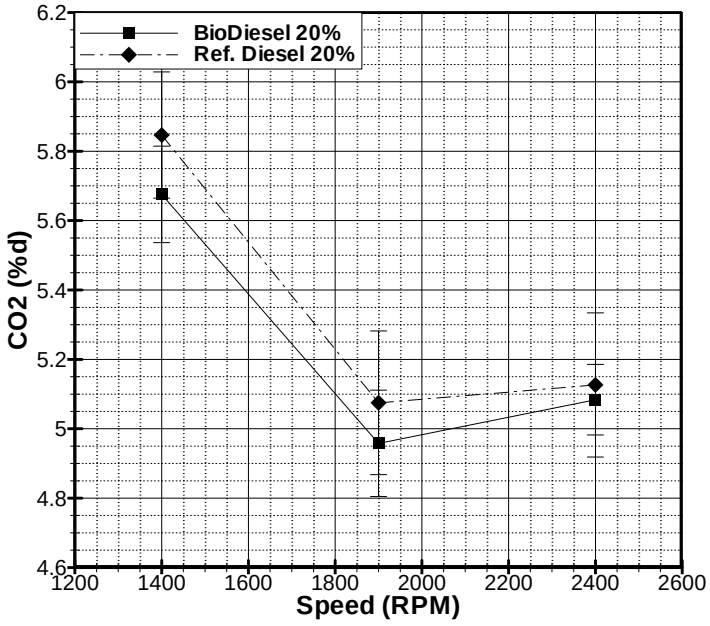

Figure 36: CO_2 at 20% Load vs. Speed

Figure 36 displays the CO_2 percentages found in the exhaust of both fuels at 20 percent load. The CO_2 falls as speed increases until the engine reaches 2400 rpm, where there is a slight rise from the 1900 rpm. The B100 has lower averages than the ULS, but no statistical difference at low loads.

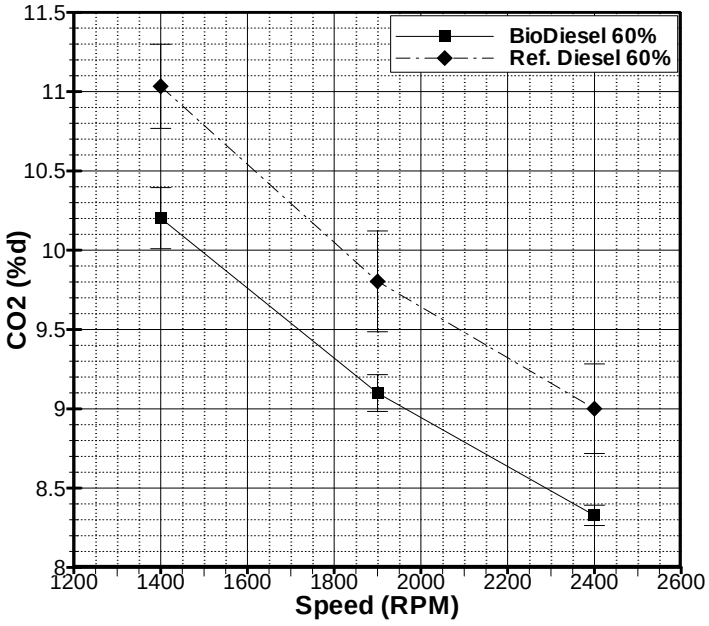

Figure 37: CO_2 at 60% Load vs. Speed

Unlike Figure 36, Figure 37 has higher CO_2 concentrations and the concentration falls as the speed increases. Also there is a major statistical difference here as more of a load is placed on the engine.

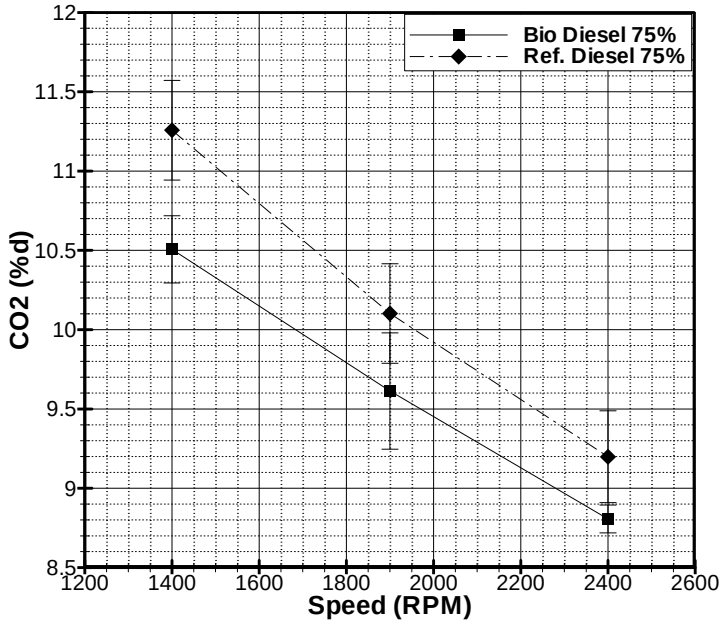

Figure 38: CO_2 at 75% Load vs. Speed

The CO_2 rises as the load rises for each individual speed, as seen in Figure 36, Figure 37, and Figure 38. For the mid to high load conditions the percentage decreases as the speed increases. There is only a statistical difference at the 20 and 75 percent load.

Previous studies have come up with similar results stating that 100 percent biodiesel has a lower carbon content, and this is the reason for lower O_2 emissions [16]. The carbon content ranges from 52.2 to 77 percent carbon for 100 percent biodiesels, while diesel has a carbon percentage of 87 percent, and the ULS has a carbon percentage of 86.9 percent. The lower carbon content along with the fact that the B100 contains oxygen and runs leaner is the reason why the CO_2 concentrations are lower for the B100.

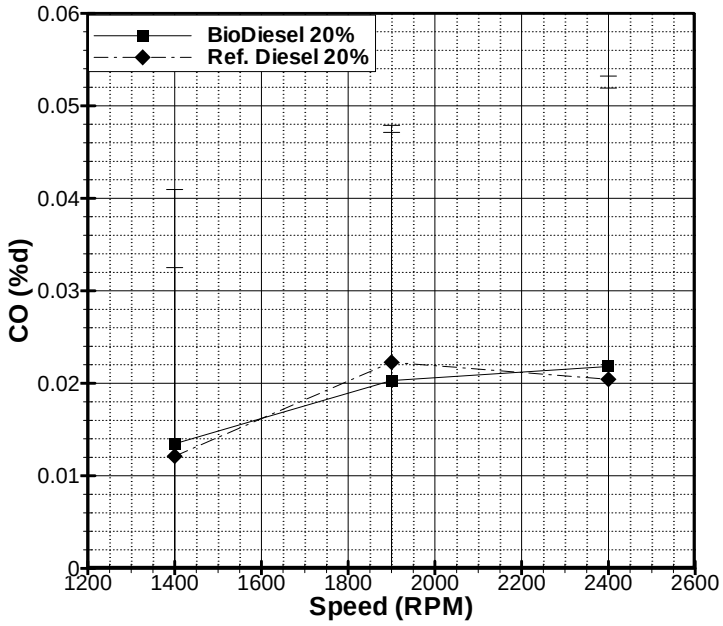

Figure 39: CO at 20% Load vs. Speed

CO concentrations are displayed in Figure 39, Figure 40, and Figure 41. The CO emissions show no variance between the two fuels at 20 percent load during all speeds in Figure 39. There is a slight rise as the speed increases. As the load increased there is a minimal separation of the two fuels CO emissions in Figure 40.

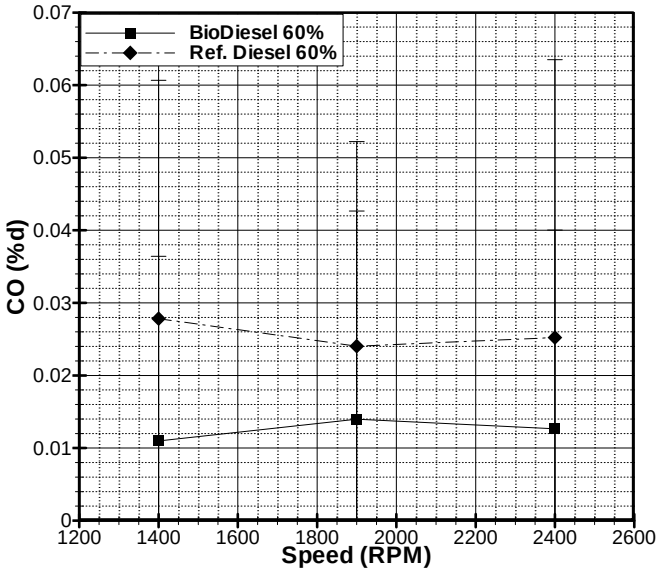

Figure 40: CO at 60% Load vs. Speed

.

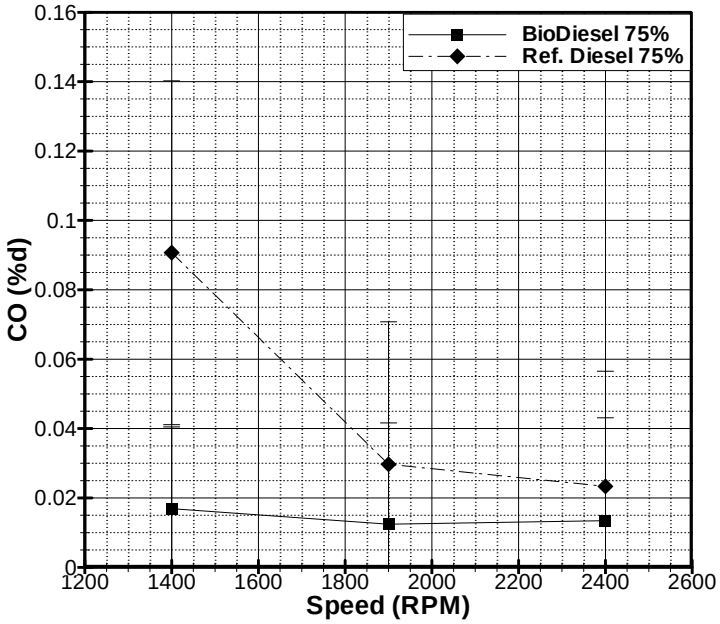

Figure 41: CO at 75% Load vs. Speed

Figure 41 shows the largest quantity difference than the previous CO emissions at 1400 rpm. Like Figure 40 the B100 emits the lowest amount of carbon monoxide at all three speeds.

CO is a minor problem for diesel engines for the fact that diesels operate with lean combustion, therefore having more than enough O_2 to oxidize most of the CO into CO_2. Comparable results were found by Lin et al, [16]. That study accredited the lower CO emissions to biodiesel having superior combustion due to the fact that it is a more oxygenated fuel; the same was also mentioned by Alam et al, [17].

Now that the O_2, CO_2, and CO has been analyzed, the last set of emission data that was taken was the NO concentrations. As mentioned earlier the NO concentrations are important because they are one of the most stringent regulated emissions of combustion engines. This is because of the troposheric ozone formation and acid rain production caused by NO_x. Before concentrating on the NO the dilution ratio, and EGR mass fraction will be analyzed first, since EGR is a method to control or reduce NO_x concentrations. The dilution ratio was used to calculate the EGR mass fraction that is present in the intake for each speed and load. The amount of EGR that the engine has in the intake is important because EGR is a method that is used to control or reduce the amount of NO_x emitted by the engine. In Figure 42, Figure 43, and Figure 44 the dilution ratio for all three loads are shown.

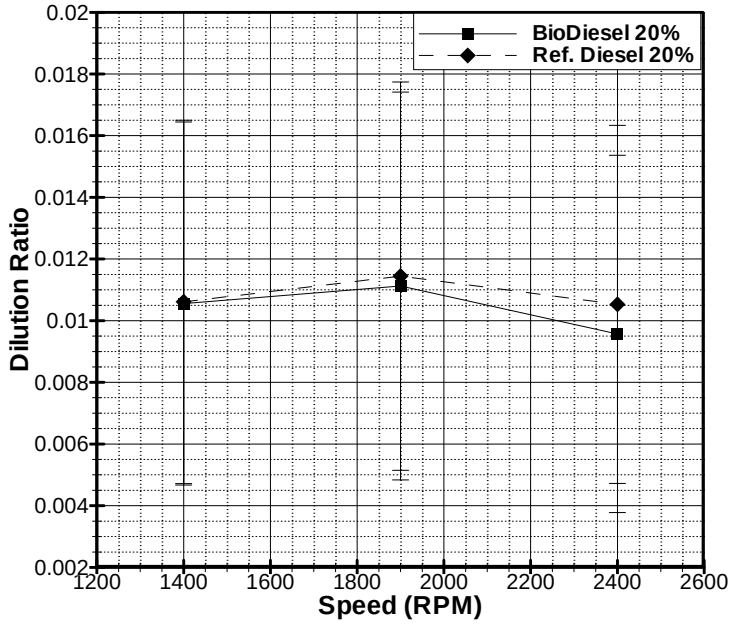

Figure 42: Carbon Dioxide Dilution Ratio at 20% Load vs. Speed

At 20 percent load there is hardly and stress placed o the engine. There is no CO_2 flowing in the intake from the exhaust at 20 percent load. The averages for both fuels are almost the same until 2400 rpm, and there is no statistical difference between the two fuels at any speed.

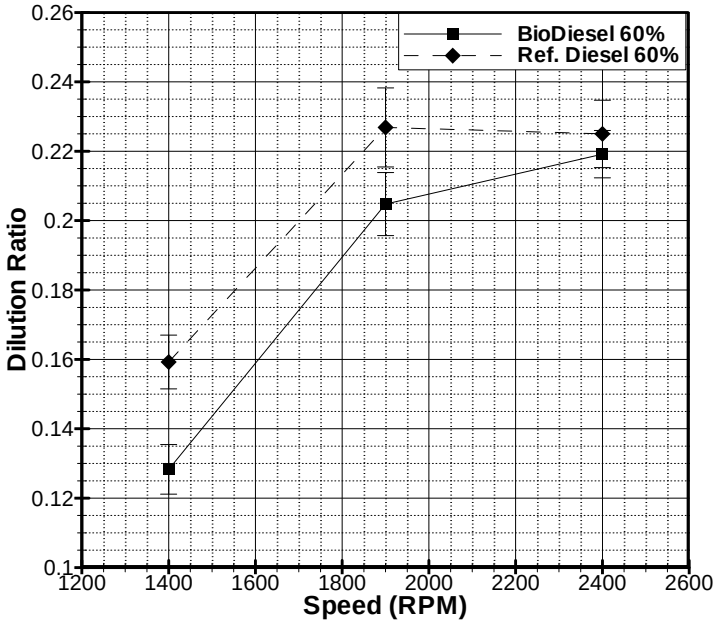

Figure 43: Dilution Ratio at 60% Load vs. Speed

Figure 43 shows the dilution ratio at 60 percent load. It is here where the first signs of EGR appear in this test, and there is an actual difference in the data, except for at high speeds. The CO_2 increases as the load increases except for the ULS at 2400 rpm, and the B100 averages less carbon dioxide in the intake than the ULS at all speeds.

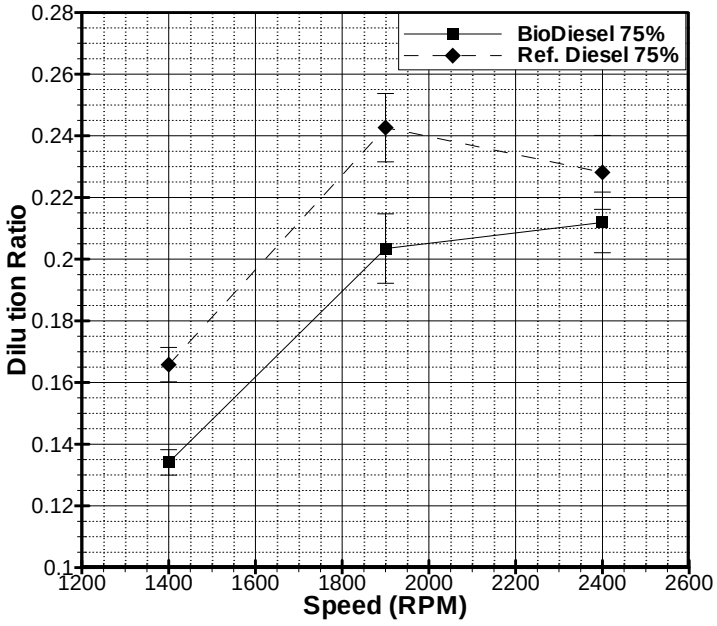

Figure 44: Dilution Ratio at 75% Load vs. Speed

It is here at 75% there is more separation between the two fuels at the low and mid speeds, and just like Figure 43 there is no statistical difference at the high speed condition.

As stated earlier the EGR flow rate is delegated by the engine's ECU. These figures do give some insight to the carbon dioxide percentages in the exhaust. Figure 45, Figure 46, and Figure 47 will show the EGR mass fractions calculated from the dilution ratio.

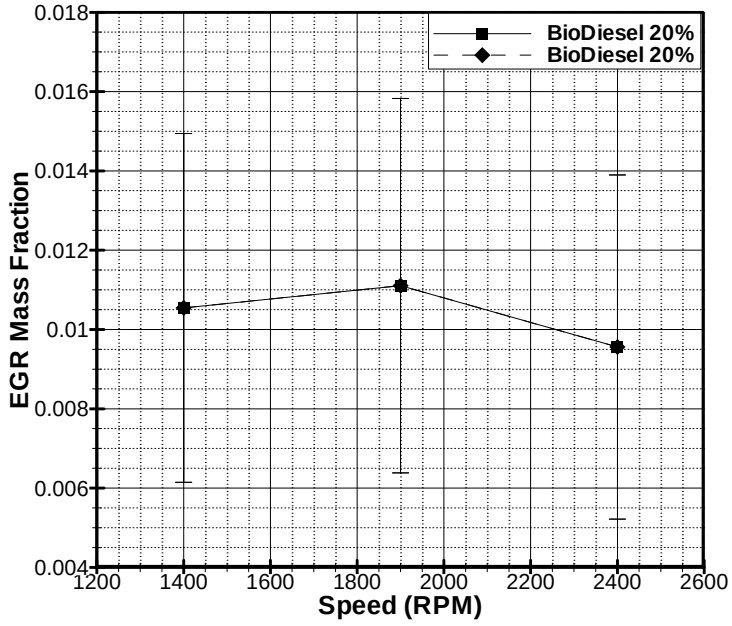

Figure 45: EGR Mass Fraction vs. Speed at 20% Load

At 20 percent load there is no EGR being used by the engine, and both fuels show the same level of EGR at all speeds.

Figure 46 shows the first sign of EGR. The 60 percent load condition is where the engine first reaches 170 degree Fahrenheit. As shown in the figure above EGR is present at all three speeds.

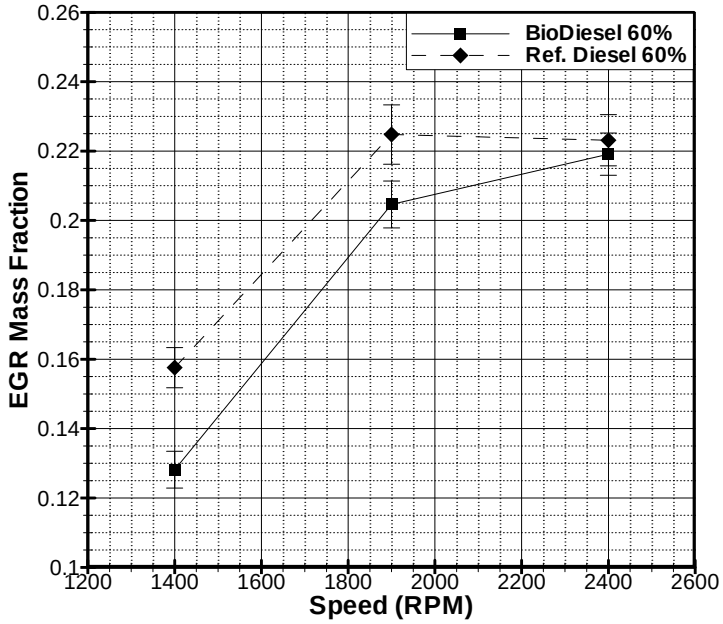

Figure 46: EGR Mass Fraction vs. Speed at 60% Load

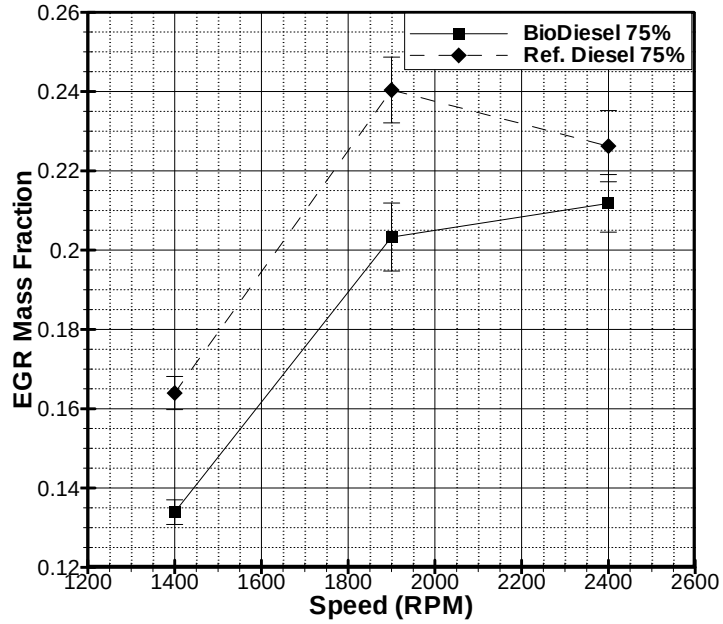

Figure 47: EGR Mass Fraction vs. Speed at 75% Load

Figure 47 shows the EGR mass fraction at 75 percent load. It is here where the most EGR is flowing at the mid range speed for the ULS diesel, while the B100 has the same amount here as in Figure 46.

The ULS averages more EGR flow when EGR is present but only has a statistical difference at 1400 and 1900 rpm. The EGR mass fraction averages the most at the mid range speed for both 60 and 75 percent when EGR is present in the intake manifold. Next the NO concentrations will be displayed in Figure 48, Figure 49, and Figure 50 to show how EGR affects the NO concentrations behavior of the engine.

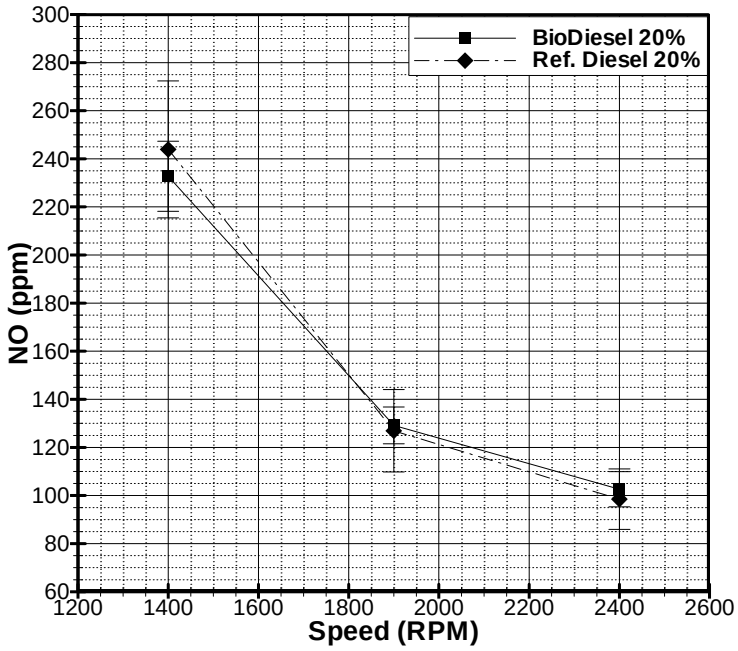

Figure 48: NO at 20% Load vs. Speed

Figure 48 shows the NO concentrations at 20 percent load, the parts per million are practically the same for both fuels. NOx concentrations descend as the speed rises.

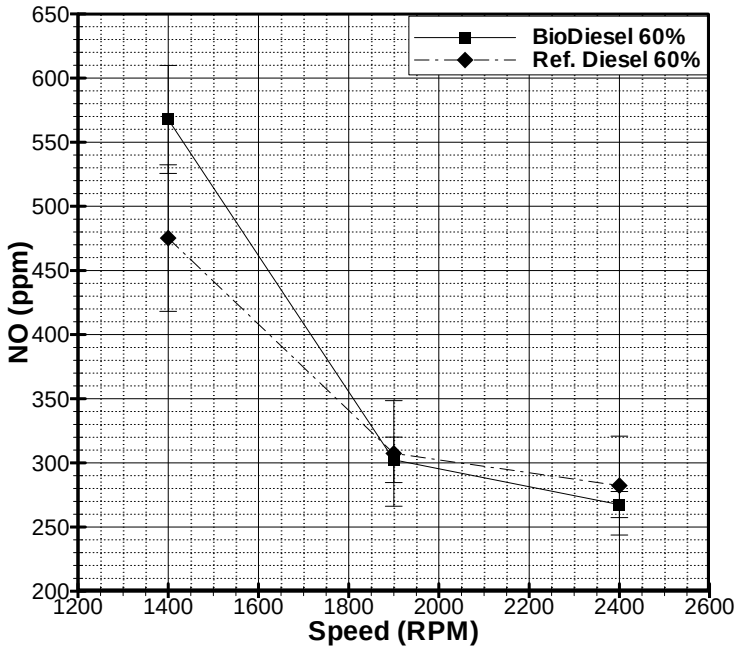

Figure 49: NO at 60% Load vs. Speed

Figure 49 follows the same pattern as Figure 48, but the B100 emits about 100 ppm more than the ULS at 1400 rpm for 60 percent load. There is a difference in the averages at 1400 rpm, but there is not a statistical difference within a 95% confidence range. The B100 has a slightly higher NO concentration at the lower speeds, and lower emissions at the highest speed.

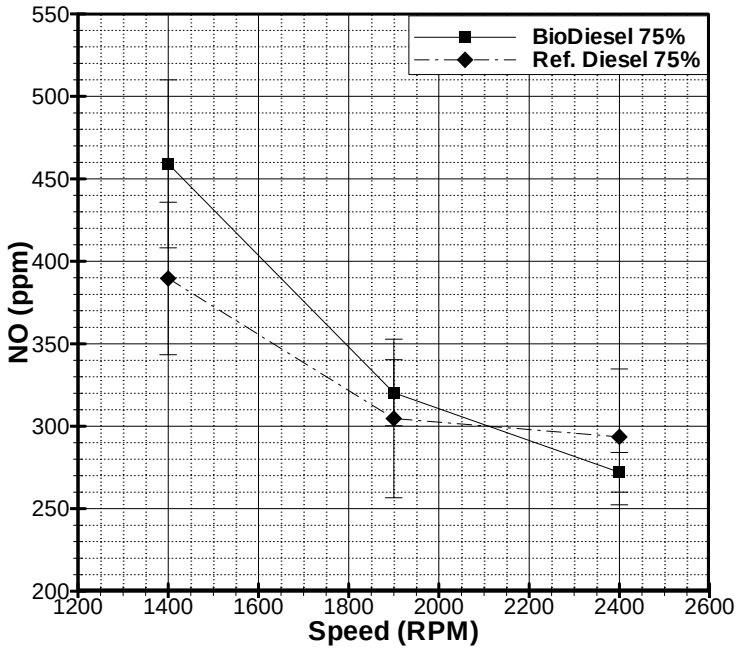

Figure 50: NO at 75% Load vs. Speed

Figure 48, Figure 49, and Figure 50 all show the same pattern in NO concentrations with the mid and high load condition emitting the most NO. Notice that the NO concentrations fall as speed rises in the 20 percent load condition even though there is no EGR (see Figure 42, and Figure 45), so the increase in speed alone is enough to lower NO concentration. The increasing speed takes time away from the heat from combustion to transfer to the N_2 and O_2 so they can form NO. This is a potential reason that less EGR can be used to control NO at 2400 rpm that at 1900 rpm as seen in Figure 46, and Figure 47. The B100 only has a noticeable average difference at 1400 rpm. Less heat transfer created by the higher speeds along with more EGR at the mid to high load conditions help to lower NOx in Figure 49, and Figure 50. The B100 contains more O_2 and therefore at lower speeds there is more opportunity for NOx formation. Biodiesel

also emits less particulate matter, which absorbs some of the heat from combustion in conventional diesel. Less particulate matter means more energy to fuel the NO_x reactions; along with low running speeds is one contributor to biodiesel NO_x Effect at 1400 rpm.

4 CONCLUSION

This research study was able to successfully characterize the engine's emissions and the difference between the ULS and the B100. The study is essential to the Advance Engine Research Laboratory in establishing a base line profile for the emissions of the engine, and giving a minor insight to the differences between emissions of the ULS and B100. It was significant to the scientific community because this is the first study to observe the behavior of a blended biodiesel used with EGR, VGT, and a common rail fuel injection system. The following conclusions can be made from this study.

4.1 ULS Certification Diesel Characterization

- Peak torque is obtained at 1900 rpm at 75 percent load. This is because the engine is not at full load.
- Fuel consumption increases with speed and load, but torque decreases after 1900 rpm. Energy from the fuel is consumed by other sources than combustions, like friction, heat transfer, and low volumetric efficiency.
- As the engine speeds up more air is taken in, causing the oxygen content in the exhaust to rise, and make the carbon dioxide emission appear to decrease, but only the molar concentrations decrease while the emission actually increase.
- Lean combustion virtually eliminates carbon monoxide emissions in diesel combustion.
- NO concentrations fall partially due to increasing EGR flow.

4.1.1 ULS vs. B100

- Biodiesel produces less torque at all speeds and loads with the same fuel flow rate because it has a lower heating value.
- The oxygen content in the B100 causes it to emit more oxygen and have lower carbon dioxide molar concentrations. The extra oxygen also causes the B100 to burn leaner than the ULS at all test conditions.
- The B100 averages lower carbon monoxide emissions, but there are no real statistical differences between the two fuels.
- The ULS has a higher concentration of carbon dioxide in the intake when there is EGR present; however this is not able to neutralize NO concentration differences between the two fuels. The lower EGR for B100 is partly a systems issue. If the ECU could be programmed to flow the same amount of EGR, it would give a better comparison of NO emissions.
- The B100 having a lower heating value poses system issues other places than just inside the cylinder. The lower EGR for B100 is partly a systems issue, if the ECU could be programmed to flow the same amount of EGR, it would give a better comparison of NO emissions.
- There is no significant difference between B100 and the ULS in NO concentrations. Only at lower speeds is there a major difference in the averages between the fuels, this maybe the result of other phenomenon, such as heat transfer changing with engine speed. The B100 has less particulate

matter than the ULS so more energy goes to nourish the NO reaction in the B100.

REFERENCES

1 Demirbas, A., 2005, "Biodiesel Production from Vegetable Oils via Catalytic and Non-Catalytic Supercritical Methanol Transesterfication Methods," Progress in Energy and Combustion Science., **31**, pp. 466-487.

2 Xiaoming, L., Yunshan, G., Sijin, W., and Xiukun, H., 2005, "An Experimental Investigation on Combustion And Emissions Characteristics of Turbo Charged DI Engines Fueled with Blends of Biodiesel," Paper presented at 2005 SAE Brasil Fuels & Lubricants Meeting, May 2005, Rio De Janiero, BRAZI, Paper No. 2005-01-2199.

3 Canakci, M., 2007, "Combustion Characteristics of a Turbocharged DI Compression Ignition Engine Fueled with Petroleum Diesel Fuels and Biodiesel," Biosource Technology, **98**, pp. 1167-1175.

4 Kegl, B., 2006, "Experimental Analysis of Injection Characteristics Using Biodiesel Fuels," Energy and Fuels, **20**, pp. 2339-2448.

5 Senatore, A., Cardone, M., Rocco, V., and Prati, M. V., 2000, "A Comparative Analysis of Combustion Process in DI Diesel Engines with Biodiesel and Diesel Fuel," Paper presented at the 2000 SAE World Congress, Detroit, MI, Paper No. 2000-01-0691.

6 Szybist, J.P., Kirby, S.R., and Boehman, A.L., 2005, "NOx Emissions of Alternative Diesel Fuels A Comparative Analysis of Biodiesel and FT Diesel," Energy and Fuels, **19**, pp. 1484-92.

7 John Deere Power Systems, Waterloo, IA, 2006, "2006 Service Manual." CD-Rom.

8 Autozine Technical School. Variable Geometry Turbocharger (VTG). Retrieved August 01, 2008, From http://www.autoezine.org/technical_school/engine/tech_engine_3.htm#VGT.

9 Stivender, D., 1971, "Development of a Fuel-Based Mass Emission Measurement Procedure," Paper presentd at the International Mid-Year Meeting, Montreal, Quebec, SAE Paper No. 710604.

10 Figliola, R. and Beasley, D., 2000, *Theory and Design for Mechanical Measurments* 3rd ed. New York: John Wiley & Sons, Inc.

11 Heywood, J., 1988. *Internal Combustion Engine Fundamental*. New York: McGraw-Hill, Inc.

12 SAE Heavy-Duty Emissions Standards Committee, "Diesel Emmission Production Audit Test Procedure," SAE J1243. Retrieved July 08, 2008, From www.sae.com.

13 Jacobs, T., Assanis, D., and Filipi, Z., 2003, "The Impact on Exhaust Gas Recirculation on Performance and Emissions of a Heavy-Duty Diesel Engine," Paper presented at 2003 SAE World Congress in Detroit, MI, Paper No. 2003-01-1068, 13.

14 Kinoshita, E., Myo, T., and Hamasaki, K., 2007, "Diesel Combustion Characteristics of Coconut Oil and Palm Oil Biodiesel," Paper presented at the Powertrain & Fluid Systems Conference and Exhibition, October 2006, Toronto, ON, Paper No. 2006-01-3251.

15 Tat, M., Van Gerpen, J., and Wang, P., 2004, "Fuel Property Effects on Injection Timing, Ignition Timing, and Oxides of Nitrogen Emissions from Biodiesel-Fueled Engines," ASABE **50**(4), pp. 1123-1128.

16 Lin, C., and Lin, H., 2007, "Diesel Engine Performance and Emission Characteristics of Biodiesel Produced by the Peroxidation Process," Fuel, **85**, pp. 298-305.

17 Alam, M., Song, J., and Acharya, R., 2004, "Combustion and Emissions Performance of Low Sulfur, Ultra Low Sulfur, and Biodiesel Blends in a DI Diesel Engine," Paper presented at the 2004 Powertrain & Fluid Systems Conference & Exhibition, October 2004, Tampa, FL, Paper No. 2004-01-3024.

18 Yamane, K., Kato, T., Okutani, H., and Shimamoto, Y., 2003, "Effect of Refining Process in Biodiesel Fuel Production on Fuel Properties, Diesel Engine Performance and Emissions," Paper presented at the 2003 JSAE/SAE International Spring Fuels and Lubricants Meeting, Yokohama, Japan, Paper No. 2003-01-1930.

19 Graboski, M., and. McCormick, R., 1998, "Combustion of Fat and Vegetable Oil Derived Fuels in Diesel Engines," Energy Combustion Science, **24**, pp. 125-64.

20 Yamane, K., Ueta, A., and Shimamoto, Y., 2001, "Influence of Physical and Chemical Properties of Biodiesel Fuels on Injection, Combustion and Exhaust Emission Characteristics in a Direct Injection Compression Ignition Engine," Int. Journal of Engine Research, **2**, pp. 249-261.

21 Karaosmanoglu, F., Baris, K., Tuter, M., and Ertekin, S., 1996, "Investigation of the Refining Step of Biodiesel," Energy and Fuels, **10**, pp. 890-895.

22 Kegl, B., and Hribernik, A., 2006, "Experimental Analysis of Injection Characteristics Using Biodiesel Fuel," Energy and Fuels, **20**, pp. 2239-2248.

23 Krahl, M., Bahadir, M, Schumacher, L., and Elser, N., 1996, "Utilization of Rapeseed Oil, Rapeseed Oil Methyl Ester or Diesel Fuel: Exhaust Gas Emissions and

Estimation of Environmental Effects," Paper presented at SAE International Fall Fuels and lubricants Meeting and Exhibition, San Antonio, Texas, Paper No. 962096.

24 Lin, C., Lin, H., and Hung, L., 2006, "Fuel Structure and Properties of Biodiesel Produced by the Peroxidation Process," Fuel, **85**, pp. 1743-1749

25 Kumar, R., and Vijayaraj, S., 2005, "Performance and Emission Analysis on a Direct Injection Diesel Engine Using Biodiesel from Palm Oil Exhaust Gas recirculation," Paper presented at ASME Internal Combustion Engine Division 2005 Fall Technical Conference September 2005, Ottawa, ON, Canada, Paper No. ICEF2005-1232.

26 Ban-Weiss, G., Chen, J., Buchholz, B., and Dibble, R., 2007, "A Numerical Investigation into Anomalous Slight NOx Increase When Burning Biodiesel; A New (Old) Theory," Fuel Processing Technology, **88**(7), pp 659-667.

27 Akasaka, Y., Suzuki, T., and Sakurai, Y., 1997, "Exhaust Emissions of a DI Diesel Engine Fueled with Blends of Biodiesel and Low Sulfur Diesel Fuel," Paper presented at SAE International Fall Fuels and lubricants Meeting and Exhibition, Tulsa, Oklahoma, Paper No. 972998.

28 Yoon, S., Park, S., Kim, D., Kwon, S., and Lee, C., 2005, "Combustion and Emission Characteristics of Biodiesel Fuels in a Common Rail Diesel Engine," Paper presented at the ASME Internal Combustion Engine Division 2005 Fall Technical Conference, Ottawa, Canada, Paper No. ICEF2005-1258.

29 Lin, C., and Lin, H., 2007, "Engine Performance and Emission Characteristics of a Three-Phase Emulsion of Biodiesel Produced by Peroxidation," Fuel Processing Technology, **88**, pp. 35-41.

30 Moshiri, M., Payne, M. and Vasquez, M., 2001, "Emission and Performance Effects of Biodiesel Blends of B5, B20 and B100 in a Single-Cylinder Medium-Speed Diesel Engine," Paper presented at ASME Internal Combustion Engine Division 2006 Spring Technical Conference May 2006, Aachen, Germany, Paper No. ICES2006-1384.

31 Cheng, A., Upatnieks, A., and Mueller, C., 2006, "Investigation of the Impact of Biodiesel Fuelling on NOx Emissions Using an Optical Direct Injection Diesel Engine," International Journal of Engine Research, **7**, pp. 297-318.

32 Monyem, A., and Van Gerpen, J., 2001, "The Effect of Biodiesel Oxidation on Engine Performance and Emissions," Biomass and Bioenergy, **20**, pp. 317-325.

33 Monyem, A., Van Gerpen, J., and Canakci, M., 2001, "The Effect of Timing and Oxidation on Emissions from Biodiesel-Fueled Engines," ASABE, **44**(1), pp. 35-42.

34 Cetinkaya, U., Tekin, Y, and Karaosmanoglu, F., 2005, "Engine and Winter Road Test Performances of Used Cooking Oil Originated Biodiesel," Energy Conservation and Management, **46**, pp. 1279-1291.

35 Demirbas, A., 2005, "Biodiesel Impacts on Compression Ignition Engine (CIE): Analysis of Air Pollution Issues Relating to Exhaust Emissions," Energy Sources, **27**, pp. 549-558.

36 Kalligeros, S., Zannikos, F., Stournas, S., and Lois, E., 2003, "An Investigation of Using Biodiesel/Marine Diesel Blends on the Performance of a Stationary Diesel Engine," Biomass and Bioenergy, **24**, pp. 141-149.

37 Lue, Y., Yeh, Y., and Wu, C., 2001, "The Emission Characteristics of a Small Direct Injection. Diesel Engine Using Biodiesel Blended Fuels," J. Enviro. Sci. Health, **A36** (5), pp. 845-859.

38 Agarwal, A., Bijwe, J., and Das, L., 2003, "Wear Assessment in a Biodiesel Fueled Compression Ignition Engine," Journal of Engineering for Gas Turbines and Power, **125**, pp. 820-826.

39 Ferguson, C., and Kirkpatrick, A., 2001, *Internal Combustion Engines* 2nd ed., John Wiley & Sons, Inc., New York.

40 Jacobs, T., Jagmin, C., Williamson, W., Fillpi, Z., Assanis, D., and Bryzik, W., "Perfomance and Enhancements of a Variable Geometry Turbocharger on a Heavy-Duty Diesel Engine," To appear in the International Journal of Heavy Vehicle Systems.

VITA

Name: Brandon T. Tompkins

Address: 2525 Pinon Ct
Bryan, TX 77802

Email Address: tompkib@tamu.edu

Education: B.S., Mechanical Engineering, Clemson University, 2005
M.S., Mechanical Engineering, Texas A&M University, 2008